AD_____
(Leave blank)

Award Number:
W81XWH-12-1-0182

TITLE:
Targeting the Prostate Cancer Microenvironment to Improve Therapeutic Outcomes

PRINCIPAL INVESTIGATOR:
Yu Sun, Ph.D.

CONTRACTING ORGANIZATION:
Fred Hutchinson Cancer Research Center
Seattle, WA 98109

REPORT DATE:

June 2013

TYPE OF REPORT:

Annual

PREPARED FOR: U.S. Army Medical Research and Materiel Command
Fort Detrick, Maryland 21702-5012

DISTRIBUTION STATEMENT: (Check one)

X Approved for public release; distribution unlimited

☐ Distribution limited to U.S. Government agencies only; report contains proprietary information

REPORT DOCUMENTATION PAGE

Form Approved
OMB No. 0704-0188

1. REPORT DATE *(DD-MM-YYYY)*	**2. REPORT TYPE**	**3. DATES COVERED** *(From - To)*
June 2013	Annual	15 May 2012–14 May 2013

4. TITLE AND SUBTITLE

Targeting the Prostate Cancer Microenvironment to Improve Therapeutic Outcomes

5a. CONTRACT NUMBER
W81XWH-12-1-0182

5b. GRANT NUMBER
W81XWH-12-1-0182

5c. PROGRAM ELEMENT NUMBER

6. AUTHOR(S)

Yu Sun, Ph.D.

5d. PROJECT NUMBER

5e. TASK NUMBER

5f. WORK UNIT NUMBER

7. PERFORMING ORGANIZATION NAME(S) AND ADDRESS(ES)

Fred Hutchinson Cancer Research Center
Seattle, WA 98109

8. PERFORMING ORGANIZATION REPORT

9. SPONSORING / MONITORING AGENCY NAME(S) AND ADDRESS(ES)

U.S. Army Medical Research
and Materiel Command
Fort Detrick, MD 21702-5012

10. SPONSOR/MONITOR'S ACRONYM(S)

11. SPONSOR/MONITOR'S REPORT NUMBER(S)

12. DISTRIBUTION / AVAILABILITY STATEMENT
Approved for public release; distribution unlimited.

13. SUPPLEMENTARY NOTES

14. ABSTRACT

Therapies designed to damage DNA (e.g. chemotherapy and irradiation) cure many primary prostate carcinomas (PCa) and produce significant responses in a subset of advanced metastatic cancers. However, a subset of localized cancers resist genotoxic treatments, and most advanced cancers treated with such therapies eventually progress to a lethal phenotype. Thus, therapy resistance is a major contributor to PCa morbidity and mortality. We want to explore the hypothesis that DNA damaging therapeutics generates responses in benign cell types comprising TME that promote tumor cell survival and enhance resistance. We have assessed the outcome of targeting individual mediators of this microenvironment-derived DDSP---specifically a member of the Wnt superfamily, WNT16B and demonstrated the highly effective neutralization of prostate cancer cell malignancy *in vitro* by purified anti-WNT16B. We anticipate that suppressing WNT16B will diminish treatment-initiated resistance, and improve *in vivo* tumor responses. We have established primary mouse prostate fibroblast cell lines and examined their responses including DDSP development upon DNA damage, and demonstrated the potential complication of regulatory mechanisms of DDSP program.

15. SUBJECT TERMS
Prostate cancer, microenvironment, DNA damage, secretion, therapy resistance, outcome.

16. SECURITY CLASSIFICATION OF:			**17. LIMITATION OF ABSTRACT**	**18. NUMBER OF PAGES**	**19a. NAME OF RESPONSIBLE PERSON** USAMRMC
a. REPORT U	**b. ABSTRACT** U	**c. THIS PAGE** U	UU	30	**19b. TELEPHONE NUMBER** *(include area code)*

Standard Form 298 (Rev. 8-98)

Table of Contents

INTRODUCTION

Current therapies designed to damage DNA (e.g. radiation therapy) cure many primary prostate carcinomas and produce significant responses in a subset of advanced metastatic cancers. However, a subset of localized prostate cancers resist genotoxic treatment, and most advanced cancers treated with chemotherapy eventually progress to a lethal phenotype. Thus, therapy resistance is a major contributor to prostate cancer morbidity and mortality. Several mechanisms responsible for resistance to genotoxic therapies have been identified and include the expression of drug efflux pumps, apoptotic deficiency, up-regulation of stress-response chaperone proteins, and enhanced mechanisms to repair mutations and DNA strand breaks. Though these mechanisms are clearly operative in a subset of tumors, *in vitro* studies of tumor cell lines poorly predict *in vivo* resistance, suggesting that cell autonomous and non-autonomous factors derived from the tumor microenvironment (TME) contribute to pro-survival effects.

We and others have identified a unique and robust secretory phenotype of prostate stromal cells as part of the response to DNA damage treatments that is termed a DNA Damage Secretory Program (DDSP). The DDSP complex is comprised of a large number of factors known to influence tumor progression and includes proteases (MMPs), growth factors (HGF, amphiregulin), pro-angiogenic factors (VEGF), and pro-inflammatory cytokines (IL6, IL8). Components of the DDSP are also capable of promoting an epithelial to mesenchymal transition (EMT), a phenotype known to enhance resistance to cytotoxic and cytostatic cancer treatments.

BODY

We propose to test the concepts that (i) genotoxic treatment, in contrast to other cancer therapeutics, produces a robust paracrine-acting secretory program (DDSP) in benign components of the TME; (ii) specific components of the DDSP activate tumor cell survival programs; and (iii) certain DDSP-activated programs (e.g. WNT signaling) can be exploited to enhance subsequent treatment responses. The following summarizes the technical objectives for the proposal and the work accomplished during the first 4-month research period between the project initiation (05/15/2012) and institution transfer of the PI (08/22/2012).

Specific Aim 1: Determine the effect and effectiveness of inhibiting WNT16B, a key component of the prostate fibroblast DNA Damage Response Program, on prostate tumor responses to chemotherapy. Through these studies, this Aim will also assess the composition of the DDSP in specific cell types comprising the prostate TME and define damage responses produced by non-genotoxic agents.

Task 1.1: Establish xenografts compring PCa cells (PC3/VCaP) with PSC27 fibroblasts and examine tumor responses to single agent or combination therapy. (y 1/m 1-6)

1. Purification, refolding, and examination of human WNT16B antibody

We wish to study the feasibility and efficacy of anti-WNT16B antibody in down-regulation of prostate tumor progression in preclinical xenograft models. Our recent data demonstrated that components of the DNA damage response program produced by benign components of the tumor microenvironment contribute to enhanced tumor repopulation rates. Particularly, the components of treatment-activated DNA damage secretory program (DDSP)—collectively or individually, alter neoplastric characteristics, for example promoting the acquisition of mesenchymal cell characteristics (epithelial to mesenchymal transition, EMT), that are known to

enhance resistance to growth arrest signals and apoptosis. The proposed work is relevant in the context of prostate cancer (PCa) treatment as one objective is to validate that key paracrine-acting molecules we have discovered, hereby exemplified by a *wingless-type MMTV integration site family member 16B*, WNT16B, which was induced 33-fold upon DNA damage, are amenable to therapeutic targeting to enhance the effectiveness of commonly used prostate cancer therapies.

Extracellular drug targets have many advantages over intracellular ones, such as easy access by small-molecule inhibitors and antibodies. WNT16B is highly expressed in PCa patients post chemotherapy, and expression has been correlated with aggressive disease (Sun et al., 2012; Sun and Nelson, 2012). Our former work showed directly that WNT16B contributes to the aggressive phenotype, and forced expression of WNT16B increased PCa cell proliferation, mobility, invasiveness, and more remarkably, chemoresistance; in contrast, knockdown of this factor by genetic strategy significantly diminished tumor development. Thus, we plan to explore the hypothesis that the DNA-damaging regimen comprising a WNT16B-directed monoclonal antibody can result in decreased cancer malignancy, which allows improving PCa treatment through such an antibody-mediated administration. Together, future experimental findings may establish WNT16B as a new, specific, and -- by virtue of its outside-of-the-box location-- druggable target for the potentially lethal forms of prostate cancer.

For this purpose, it is essential to get purified anti-WNT16B as the preliminary step of the whole project. A solubilized mouse anti-human WNT16B monoclonal antibody from a commercial source prepared in aqueous buffered solution containing ≤0.09 % sodium azide, was purified by affinity chromatography using a Sephadex G25 gel filtration column. After one-step chromatographic purification in denaturing conditions, we optimized a cost saving dialysis procedure for correct refolding (Burgess 2009; Bel-Ochi et al., 2013) to improve the specific immunoreactivity of this complex molecule. The refolding procedure consists of consecutive dialysis baths with decreasing urea concentrations. The immunoreactivity recovery was confirmed by western blot analysis with whole cell lysates from PSC27 stable line that has been established by lentiviral infection to overexpress WNT16B (**Figure 1A**). No degradation products, protein aggregates or misfolded species were detected in the buffered antibody solution, as examined by anti-mouse HRP-conjugated secondary antibody (not shown). Typically, a 0.1 ml volume of 50 μg commercial raw antibody (Clone F4-1582) led to a final yield of about 40 μg purified anti-WNT16B. This amount even exceeded the terminal production estimated by the manufacture. Thus, our methodology allowed generation of anti-WNT16B that exhibit apparent biological activities and yielded sufficient products for downstream applications.

2. Characterization of purified anti-WNT16B in phenotypic changes of PCa epithelial cells by human prostate stroma in response to DNA damage insults

To confirm the efficacy of anti-WNT16B generated through such a series of purification and recovery procedures, we applied the antibody to *in vitro* experiments. First, we looked at the influence of the antibody in affecting the proliferative augment gained by WNT16B as an overexpressed soluble factor from the PSC27-WNT16B stable cell line. As compared with the buffer control, solutions containing purified anti-WNT16B significantly reduced the growth potential of BPH1, M12 and PC3 cells conferred by conditional media from stromal cells, although the effect to PC3 cells was most dramatic (**Figure 1B**).

As one of the prominent features of a full fibroblast DDSP program, conditional media from damaged fibroblasts upon ionizing radiation (PSC27-RAD) can stimulate the proliferation of neoplastic prostate cells. However, this was found to be significantly attenuated by antibody-

mediated suppression (**Figure 1C**). Further, the enhanced invasive capacity of cancer epithelial cells by the full spectrum paracrine-acting fibroblast DDSP spurred by DNA damaging treatment (PSC27-RAD), was remarkably suppressed by the presence of purified anti-WNT16B (**Figure 1D**).

Task 1.3: Develop a system for studying signal transduction programs and other components of the TME regulated by WNT16B in the context of an intact immune response. (y 2/m 1-6)

3. Isolation, establishment and characterization of primary prostate fibroblast lines from the FVB mouse strain

To examine the effects of WNT16B on tumor growth and therapy resistance, and clarify signal transduction programs and other components of the tumor microenvironment (TME) regulated by WNT16B in an intact immune system, primary mouse prostate stromal cells particularly fibroblast cells are highly desired and will serve as a baseline for future xenograft expertments. This will allow replication of the cell recombination renal capsule xenograft studies (EXP1), substituting Myc-CaP (Watson et al., 2005) mouse prostate cancer cell lines and the prospective mouse fibroblasts engineered to overexpress or suppress WNT16B in the context of mitoxantrone (MIT) therapy. Myc-CaP tumor cells will allow for grafting in syngeneic *immune-intact* mouse hosts (e.g. FVB for Myc-CaP) to assess for possible immune regulatory influences of WNT16B in the TME that could enhance, or suppress WNT16B tumor effects.

For this purpose, we derived primary mouse prostate fibroblasts from wild type FVB mice at the age of 3~4 months (puberty). Nutrient specificity, morphology and growth pattern of these primary fibroblasts were characterized. For optimization of the mouse fibroblasts (MFs) culture, we tested several conditions such as DMEM versus DMEM/F12, F-10 Nutrient Mixture, Ham's F12 Nutrient Mixture, α-MEM with or without bFGF and StemXVivo medium (Sung et al., 2008; Futami et al., 2012). When the MFs were maintained with enriched culture media, such as DMEM/F12 or α-MEM with or without bFGF, cell proliferation was inadequate and cell morphology changed to flat, enlarged shapes (data not shown). However, with the routine DMEM medium the results improved with an adequate volume of cells and normal morphology. It is noteworthy that the initial culture of the isolated MFs had a heterogeneous cell population with both round and fibroblastic cells. However, the number of round-shaped cells gradually decreased and the growth rate of the fibroblastic cells increased over time upon sequential subculture. Generally, the MFs isolated from the prostate tissues of FVB mouse strain showed fibroblastic morphology (**Figure 2**). The morphologic characteristics of the MFs were similar to NIH3T3, an established mouse embryonic fibroblast line from ATCC. However, the average growth rates of the MFs were even higher. In addition, colony-forming unit fibroblast (CFU-F) numbers were used to compare various growth potentials among the fibroblasts from different sources (Sung et al., 2008). To estimate the CFU-F number, 1000 cells were plated onto a 100-cm^2 dish, and then cultured for 7 days. One subline of MFs, F4M2 showed the highest number of CFU-Fs (**Figure 3A**). Therefore, our results suggest that F4M2 is a mouse fibroblast line that can be potentially suitable for *in vitro* studies of cell biology and *in vivo* application of tumor xenografting experiments.

For molecular identification of these cell lines, whole cell lysates were collected from culture and applied for immunoblot analysis. Interestingly, the fibroblast-specific markers, including vimentin and α-SM actin were consistently expressed in the established lines, with F4M2 examined as a representative, while the typical luminal epithelial markers mainly E-cadherin and CK8 are basically missing (**Figure 3B**). This is in line with NIH3T3 cells, which is well known for its fibroblast feature, although from a different mouse strain. Thus, the expression profile of

our primary mouse prostate fibroblasts is confirmed, which appears unique and distinct from the well-established mouse prostate cancer cells of the same genetic origin (FVB).
In addition, we determined the response of F4M2 cells upon ionizing radiation. Not surprisingly, multiple secreted factors as hallmark of typical DDSP phenotype that was reported in human fibroblasts were markedly enhanced within 10 days post DNA damage (**Figure 3C**). However, the increased expression of a few soluble factors, particularly SPINK1, CXCL14 and CCL26 remained largely undiminished, when the mTOR suppressor RAD001 was applied to the culture conditions. Thus, in the presence of a small molecule inhibitor of DDSP, part of the whole range of secretion is unaffected, indicating the complexity of this fibroblast-specific program and the necessity to further explore the multiple mechanisms of DDSP development, some of which are so far still cryptic and unclear.

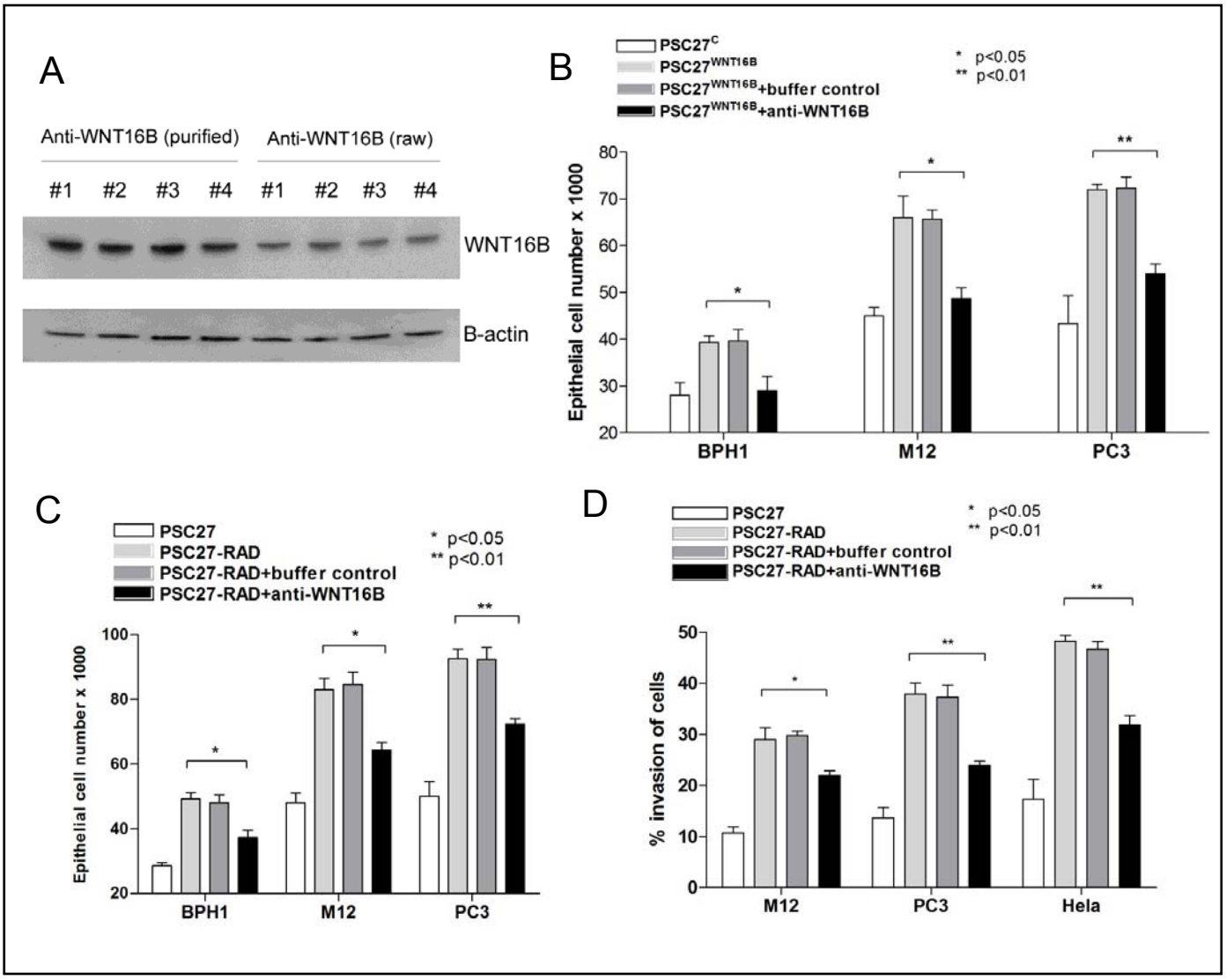

Figure 1. Purification and *in vitro* efficacy of anti-WNT16B (clone F4-1582) through co-culture examination. **A.** Western blot assay of whole cell lysates collected from PSC27-WNT16B stable line, probed with anti-WNT16B purified from a column chromatography, with the same antibody without purification applied as parallel control. Loading amount of cell lysates per lane, 20 μg; concentrations of antibody (representative of multiple times of preparation for lane 1~4, or corresponding lots of raw commercial antibody for lane 5~6), 2.5 μg/10 ml. WNT16B was identified as a single band of ~45 kDa. **B.** Conditional media from WNT16B-expressing prostate fibroblasts promotes PCa epithelial cell proliferation. However, this tendency is diminished by anti-WNT16B. **C.** A full fibroblast DDSP program induced by ionizing radiation (PSC27-RAD) stimulates the proliferation of neoplastic prostate cells, but is significantly attenuated by antibody-mediated suppression. **D.** The entire paracrine-acting fibroblast DDSP spurred by DNA

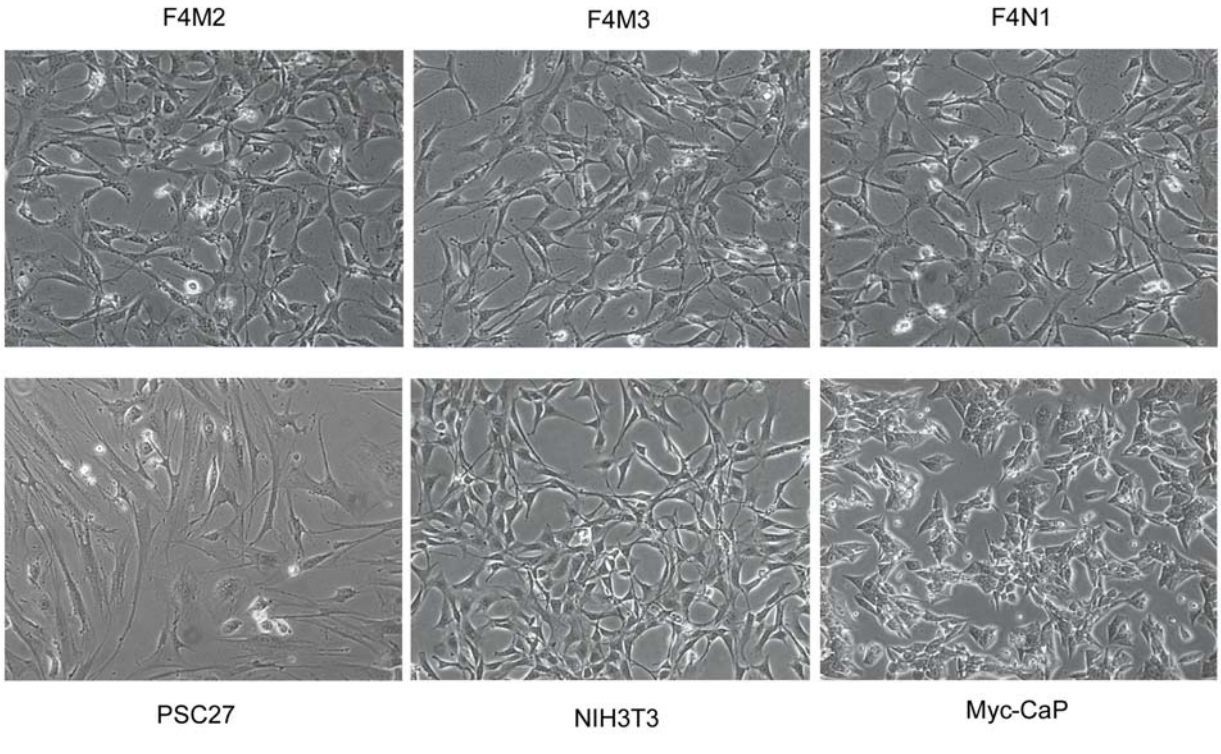

Figure 2. Cell morphology of primary prostate fibroblast lines isolated from FVB mice. Bright field microscopic images of 3 representatives of such cell lines are shown, and cells are maintained in optimized culture media. Among them, F4M2 grows faster than others, and all three lines resemble NIH3T3, a well-established and widely used mouse embryonic fibroblast line. The primary normal human prostate stromal line, and Myc-CaP line originally derived from mouse High-Myc transgenic model of prostate cancer, either cultured in DMEM/10%FBS, serve as parallel controls.

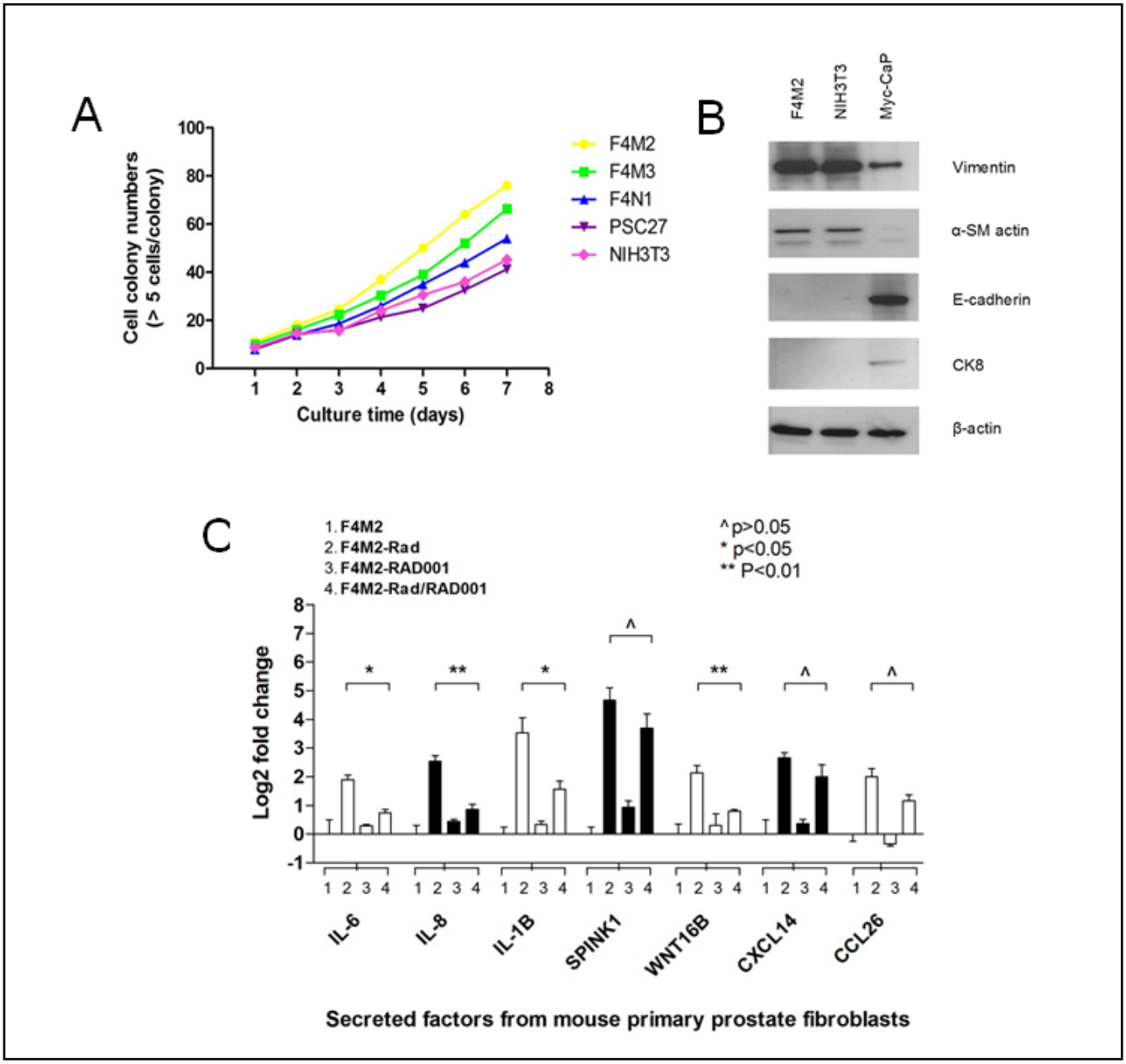

Figure 3. Growth potential and expression pattern of cell line specific markers. **A.** Colony-forming unit (CFU) is counted for cell lines cultured under the optimized conditions, in a consecutive 7-day period. To estimate the CFU number (>5 cells/colony), 1000 cells are plated onto a 100-cm^2 dish, with media changed every 2~3 days. One subline of MFs, F4M2 exhibited the highest number of CFUs. **B.** Western blots of cell lines with antibodies against seveal cell lineage specific markers applied. Actin, loading control for signal normalization. **C.** Expression profile of several typical DDSP factors in F4M2 line upon DNA damage, but their expression is differentially reduced by a chemical drug, RAD001. Note, the expression of SPINK1, CXCL14 and CCL26 promoted by genotoxicity, cannot be completely blocked upon RAD001 treatment, making them unique among multiple DDSP factors.

Specific Aim 2: Identify key upstream 'master regulators' of the DNA Damage Secretory Program and assess the anti-tumor effects of broad DDSP suppression. Through these studies the effects of the composite DDSP will be defined using 3D assays of cytotoxicity and preclinical model systems.

Not initiated yet, therefore data unavailable.

KEY RESEARCH ACCOMPLISHMENTS

- We have purified anti-WNT16B mouse monoclonal antibody through column chromatography technique and renaturing procedures. The *in vitro* experiments demonstrated that the antibody is biologically active and has even higher capacity in recognizing WNT16B as an antigen expressed from human fibroblasts.
- Upon application to cell culture conditions, anti-WNT16B significantly reduced the proliferative gain of prostate cancer epithelial cells conferred by WNT16B overexpressed from a stable human fibroblast line; dramatically neutralized the growth augment exerted by the full DDSP of damaged prostate fibroblasts; and prominently abolished the invasiveness of cancer cells upon treatment with conditional media of fibroblasts upon DNA damaging.
- We isolated and established a group of primary fibroblast cell lines from the prostate tissue of mice with FVB background. Expression of the typical cell lineage-specific markers confirmed their stromal origin, and typical DDSP phenotype is developed upon DNA damaging treatment. However, as is reminiscent of our previous data from human fibroblasts, the upregulation of a handful DDSP effectors persisted even overexpression of majority of soluble factors is suppressed by pathway-targeting chemicals, imply the highly complex nature of this program and complication of a large molecular network that is engaged in the initiation and maintenance of this stroma-specific response under chemotherapy or radiation conditions.

REPORTABLE OUTCOMES

- **Sun, Y.** and Nelson, P. S. 2012. Molecular Pathways: Involving Microenvironment Damage Responses in Cancer Therapy Resistance. ***Clin Cancer Res.*** 18: 4019-4025.
- **Sun, Y.**, Campisi, J., Higano, C., Beer, T. M., Porter, P., Coleman, I., True, L. and Nelson, P. S. 2012. Treatment-Induced Damage to the Tumor Microenvironment Promotes Prostate Cancer Therapy Resistance through WNT16B. ***Nat. Med.*** 18: 1359-1368. (Article featured by the journal, reviewed by Cancer Biology & Therapy, Cancer Discovery, Nature Medicine, and Nature Reviews Clinical Oncology)

CONCLUSIONS

The research accomplished to date has demonstrated that anti-WNT16B can be purified from commercial vials supplied by the vendor, and the refolding process we've adapted from former literature allows a nearly complete recovery of its biological activities. Ac compared with the pre-purification product, anti-WNT16B demonstrated higher recognition and immunoreaction with the antigen that is expressed from human prostate stromal cells. We isolated and established primary prostate fibroblast cell lines from mice of FVB background, and characterized the expression pattern of cell lineage-specific markers, identifying these cells as typical fibroblasts per se. Upon DNA-damaging treatment, multiple DDSP factors are overexpressed significantly.

However a subgroup of the secreted factors appears to be refractory upon application of specific signaling pathway inhibitors, indicating complication of multiple mechanisms of DDSP phenotype in the tumor microenvironment.

REFERENCES

Bel-Ochi, N. C., Bouratbine, A., Mousli, M., 2013. Enzyme-Linked Immunosorbent Assay using Recombinant SAG1 Antigen to Detect Toxoplasma gondii-Specific Immunoglobulin G Antibodies in Human Sera and Saliva. Clin Vaccine Immunol. [Epub ahead of print]

Burgess, R. R. 2009. Refolding solubilized inclusion body proteins. Methods Enzymol.17: 259–282.

Cabrita, L. D. and Bottomley, S. P. 2004. Protein expression and refolding—a practical guide to getting the most out of inclusion bodies. Biotechnol. Annu. Rev.10: 31–54.

Futami, I., Ishijima, M., Kaneko, H., Tsuji, K., Ichikawa-Tomikawa, N., Sadatsuki, R., Muneta, T., Arikawa-Hirasawa, E., Sekiya, I. and Kaneko, K. 2012. Isolation and Characterization of Multipotential Mesenchymal Cells from the Mouse Synovium. PLoS One. 7: e45517.

Gilbert, L. A. and Hemann, M. T. 2010. DNA damage-mediated induction of a chemoresistant niche. Cell. 143: 355-366.

Sung, J. H., Yang, H. -M., Park, J. B., Choi, G. -S., Joh, J. -W., Kwon, C. H., Chun, J. M., Lee, S. -K. and Kim, S. -J. 2008. Isolation and Characterization of Mouse Mesenchymal Stem Cells. Transplantation Proceedings. 40: 2649–2654.

Watson, P. A., Ellwood-Yen, K., King, J. C., Wongvipat, J., Lebeau, M. M. and Sawyers, C. L. 2005. Context-dependent hormone-refractory progression revealed through characterization of a novel murine prostate cancer cell line. Cancer Res. 65: 11565-11571.

APPENDICES

See attached.

nature medicine

Treatment-induced damage to the tumor microenvironment promotes prostate cancer therapy resistance through WNT16B

Yu Sun[1], Judith Campisi[2,3], Celestia Higano[4,5], Tomasz M Beer[6,7], Peggy Porter[1], Ilsa Coleman[1], Lawrence True[8] & Peter S Nelson[1,4,5,8]

Acquired resistance to anticancer treatments is a substantial barrier to reducing the morbidity and mortality that is attributable to malignant tumors. Components of tissue microenvironments are recognized to profoundly influence cellular phenotypes, including susceptibilities to toxic insults. Using a genome-wide analysis of transcriptional responses to genotoxic stress induced by cancer therapeutics, we identified a spectrum of secreted proteins derived from the tumor microenvironment that includes the Wnt family member wingless-type MMTV integration site family member 16B (WNT16B). We determined that *WNT16B* expression is regulated by nuclear factor of κ light polypeptide gene enhancer in B cells 1 (NF-κB) after DNA damage and subsequently signals in a paracrine manner to activate the canonical Wnt program in tumor cells. The expression of WNT16B in the prostate tumor microenvironment attenuated the effects of cytotoxic chemotherapy *in vivo*, promoting tumor cell survival and disease progression. These results delineate a mechanism by which genotoxic therapies given in a cyclical manner can enhance subsequent treatment resistance through cell nonautonomous effects that are contributed by the tumor microenvironment.

A major impediment to more effective cancer treatment is the ability of tumors to acquire resistance to cytotoxic and cytostatic therapeutics, a development that contributes to treatment failures exceeding 90% in patients with metastatic carcinomas[1]. Efforts focused on circumventing cellular survival mechanisms after chemotherapy have defined systems that modulate the import, export or metabolism of drugs by tumor cells[2–6]. Enhanced damage repair and modifications to apoptotic and senescence programs also contribute to *de novo* or acquired tolerance to anti-neoplastic treatments[3,7,8]. In addition, the finding that *ex vivo* assays of sensitivity to chemotherapy do not accurately predict responses *in vivo* indicate that tumor microenvironments also contribute substantially to cellular viability after toxic insults[9–11]. For example, cell adhesion to matrix molecules can affect life and death decisions in tumor cells responding to damage[12–14]. Further, the spatial organization of tumors relative to the vasculature establishes gradients of drug concentration, oxygenation, acidity and states of cell proliferation, each of which may substantially influence cell survival and the subsequent tumor repopulation kinetics[15,16].

Most cytotoxic agents selectively target cancers by exploiting differential tumor cell characteristics, such as high proliferation rates, hypoxia and genome instability, resulting in a favorable therapeutic index. However, cancer therapies also affect benign cells and can disrupt the normal function and physiology of tissues and organs. To avoid host lethality, most anticancer regimens do not rely on single overwhelming treatment doses: both radiation and chemotherapy are administered at intervals to allow the recovery of vital normal cell types. However, gaps between treatment cycles also allow tumor cells to recover, activate and exploit survival mechanisms and resist subsequent therapeutic insults.

Here we tested the hypothesis that treatment-associated DNA damage responses in benign cells comprising the tumor microenvironment promote therapy resistance and subsequent tumor progression. We provide *in vivo* evidence of treatment-induced alterations in tumor stroma that include the expression of a diverse spectrum of secreted cytokines and growth factors. Among these, we show that *WNT16B* is activated in fibroblasts through NF-κB and promotes an epithelial to mesenchymal transition (EMT) in neoplastic prostate epithelium through paracrine signaling. Further, WNT16B, acting in a cell nonautonomous manner, promotes the survival of cancer cells after cytotoxic therapy. We conclude that approaches targeting constituents of the tumor microenvironment in conjunction with conventional cancer therapeutics may enhance treatment responses.

RESULTS

Therapy induces damage responses in tumor microenvironments

To assess for treatment-induced damage responses in benign cells comprising the tumor microenvironment, we examined tissues collected before and after chemotherapy exposure in men with prostate

[1]Division of Human Biology, Fred Hutchinson Cancer Research Center, Seattle, Washington, USA. [2]Buck Institute for Research on Aging, Novato, California, USA. [3]Lawrence Berkeley National Laboratory, Berkeley, California, USA. [4]Division of Clinical Research, Fred Hutchinson Cancer Research Center, Seattle, Washington, USA. [5]Department of Medicine, University of Washington, Seattle, Washington, USA. [6]Division of Hematology and Medical Oncology, Oregon Health and Science University, Portland, Oregon, USA. [7]Knight Cancer Institute, Oregon Health and Science University, Portland, Oregon, USA. [8]Department of Pathology, University of Washington, Seattle, Washington, USA. Correspondence should be addressed to P.S.N. (pnelson@fhcrc.org).

Received 25 April 2011; accepted 8 June 2012; published online 5 August 2012; doi:10.1038/nm.2890

cancer enrolled in a neoadjuvant clinical trial combining the genotoxic drug mitoxantrone (MIT) and the microtubule poison docetaxel (DOC) (**Fig. 1a**)[17,18]. After chemotherapy, we found evidence of DNA damage in fibroblasts and smooth muscle cells comprising the prostate stroma, as determined by the phosphorylation of histone H2AX on Ser139 (γ-H2AX) (**Fig. 1b**). To ascertain the molecular consequences of DNA damage in benign cells, we treated primary prostate fibroblasts (PSC27 cells) with MIT, bleomycin (BLEO), hydrogen peroxide (H_2O_2) or gamma radiation (RAD), each of which substantially increased the number of γ-H2AX foci (**Supplementary Fig. 1a**,**b**). We used whole-genome microarrays to quantify transcripts in PSC27 cells and determined that the levels of 727 and 329 mRNAs were commonly increased and decreased, respectively (false discovery rate of 0.1%), as a result of these genotoxic exposures (**Supplementary Fig. 1c**). To focus our studies on those factors with the clear potential for paracrine effects on tumor cells, we evaluated genes with at least 3.5-fold elevated expression after genotoxic treatments that encode extracellular proteins, here collectively termed the DNA damage secretory program (DDSP) (**Fig. 1c**). Consistent with previous studies, transcripts encoding matrix metalloproteinases such as MMP1, chemokines such as CXCL3 and peptide growth factors such as amphiregulin were substantially elevated in PSC27 fibroblasts after genotoxic damage[19,20]. Notably, the expression of *WNT16B* increased between eightfold and 64-fold as a result of these treatments ($P < 0.005$) (**Fig. 1c**,**d**).

Wnt family members participate in well-described mesenchymal and epithelial signaling events that span developmental biology, stem cell functions and neoplasia[21]. Though little information links Wnt signaling to DNA damage responses, a previous study reported WNT16B overexpression in the context of stress- and oncogene-induced senescence[22]. We confirmed that DNA damage increased WNT16B protein expression and found elevated amounts of extracellular WNT16B in conditioned medium from prostate fibroblasts after chemotherapy or radiation (**Fig. 1e**,**f**). Transcripts encoding other Wnt family members were not substantially altered in the prostate fibroblasts we studied here (**Fig. 1g**). In contrast to the *WNT16B* responses in fibroblasts, we observed little induction of *WNT16B* expression in epithelial cells (**Fig. 1h**).

We next sought to confirm that expression of *WNT16B* is induced by genotoxic therapy *in vivo*. We used laser-capture microdissection to separately isolate stroma and epithelium and determined

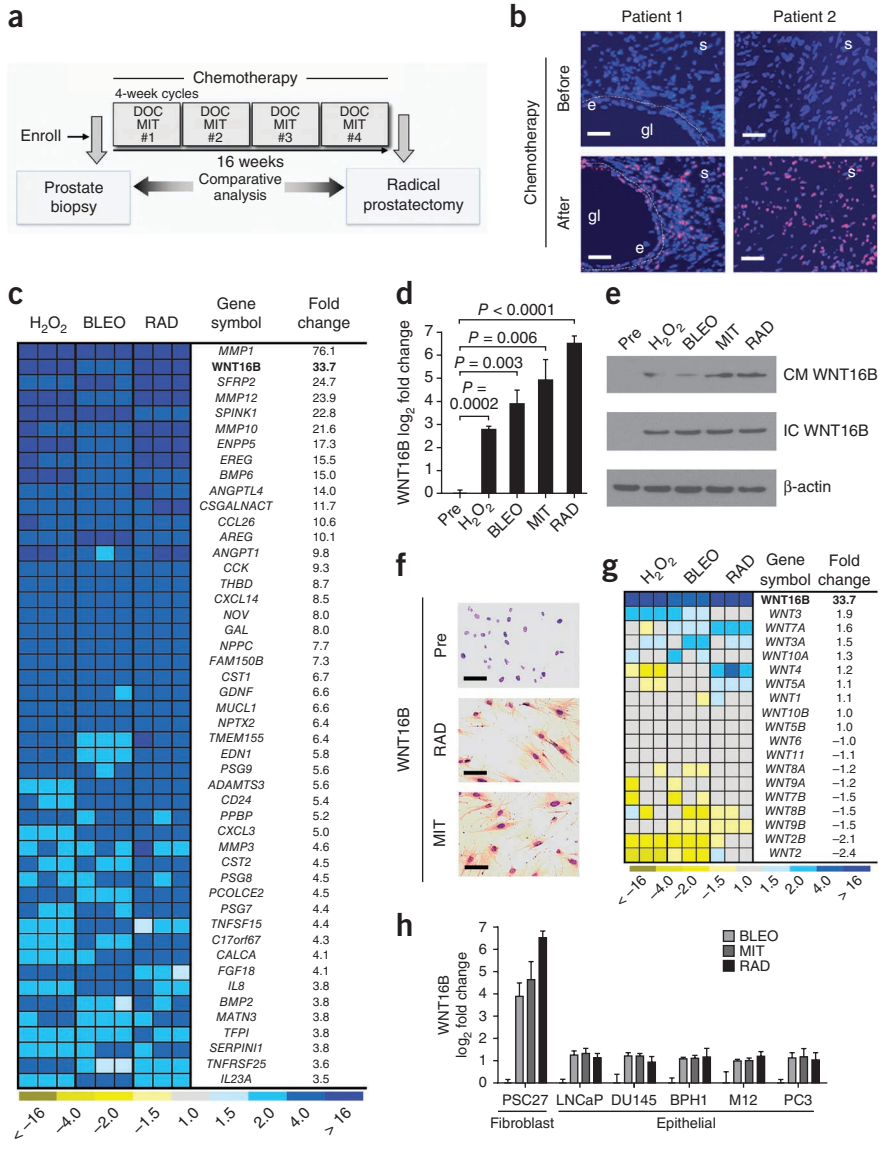

Figure 1 Genotoxic damage to primary prostate fibroblasts induces expression of a spectrum of secreted proteins that includes WNT16B. (**a**) Schematic of the prostate cancer treatment regimen comprising a pretreatment prostate biopsy and four cycles of neoadjuvant DOC and MIT chemotherapy followed by radical prostatectomy. (**b**) DNA damage foci in human prostate tissues collected before and after chemotherapy. Tissue sections were probed with antibodies recognizing γ-H2AX (red and pink signals), and nuclei were counterstained with Hoechst 33342 (blue). Gl, gland lumen; e, epithelium; s, stroma. Scale bars, 50 μm. (**c**) Analysis of gene expression changes in prostate fibroblasts by transcript microarray quantification. The heatmap depicts the relative mRNA levels after exposure to H_2O_2, BLEO or RAD compared to vehicle-treated cells. Columns are replicate experiments. *WNT16B* is highlighted in bold for emphasis. (**d**) Measurements of WNT16B expression by qRT-PCR in prostate fibroblasts. Shown are the log2 transcript measurements before (Pre) or after exposure to the indicated factors relative to vehicle-treated control cells. Data are mean ± s.e.m. of triplicates. The *P* value was calculated by analysis of variance (ANOVA) followed by *t* test. (**e**) WNT16B protein expression in prostate PSC27 fibroblast extracellular conditioned medium (CM) or in cell lysates (IC) after genotoxic exposures. β-actin is a loading control. (**f**) Immunohistochemical analysis of WNT16B expression in prostate fibroblasts before (Pre) and after exposure to MIT or RAD. Brown chromogen indicates WNT16B expression. Scale bars, 50 μm. (**g**) Expression of Wnt family members in prostate fibroblasts after exposure to DNA-damaging agents. Transcript quantification was determined by microarray hybridization. Columns represent independent replicate experiments. *WNT16B* is listed in bold for emphasis. (**h**) WNT16B expression by qRT-PCR in PSC27 fibroblasts and prostate cancer cell lines after the indicated genotoxic exposure relative to pretreatment transcript amounts. Data are mean ± s.e.m.

by quantitative RT-PCR (qRT-PCR) that the number of *WNT16B* transcripts increased by approximately sixfold in prostate stroma after chemotherapy ($P < 0.01$) (**Fig. 2a** and **Supplementary Fig. 1d**). The expression of other genes known to respond to DNA damage, including *CDKN2A* (also known as *p16*), *CDKN1A* (also known as *p21*) and *IL8*, also increased in response to chemotherapy in prostate stroma (**Fig. 2a**)[20,23]. We next confirmed induction of WNT16B protein expression by immunohistochemistry. Compared to untreated prostate tissue, WNT16B protein was substantially and significantly increased after chemotherapy in the periglandular stroma, which included fibroblasts and smooth muscle cells ($P < 0.01$) (**Fig. 2b**,**c**). In contrast, we observed very limited WNT16B expression in benign or neoplastic epithelium, and mRNAs encoding other Wnt family proteins were not substantially altered in prostate stroma (**Supplementary Fig. 1d**,**e**).

We confirmed these findings in breast and ovarian carcinomas, two other malignancies commonly treated with cytotoxic chemotherapy. Genotoxic treatments induced the expression of WNT16B protein in primary human fibroblasts isolated directly from breast and ovarian tissues and in the prostates, breasts and ovaries of mice treated with MIT (**Supplementary Fig. 2a–d**). WNT16B protein expression was significantly elevated in the stroma of human breast and ovarian cancers treated with neoadjuvant chemotherapy compared with tumors from patients that did not receive treatment ($P < 0.001$) (**Fig. 2**). Notably, in each of the tumor types evaluated, a range of absent to robust WNT16B expression was evident. Because responses to chemotherapy also varied, we evaluated whether WNT16B expression was associated with clinical outcome. In patients with prostate cancer treated with neoadjuvant chemotherapy, higher WNT16B immunoreactivity in prostate stroma after treatment was associated with a significantly greater likelihood of cancer recurrence ($P = 0.04$) (**Fig. 2d**). We next sought to determine the mechanism(s) by which WNT16B could contribute to treatment failure.

WNT16B promotes cancer cell proliferation and invasion

Members of the Wnt family influence cellular phenotypes through β-catenin–dependent and –independent pathways[21]. We generated a prostate fibroblast cell strain with stable expression of WNT16B

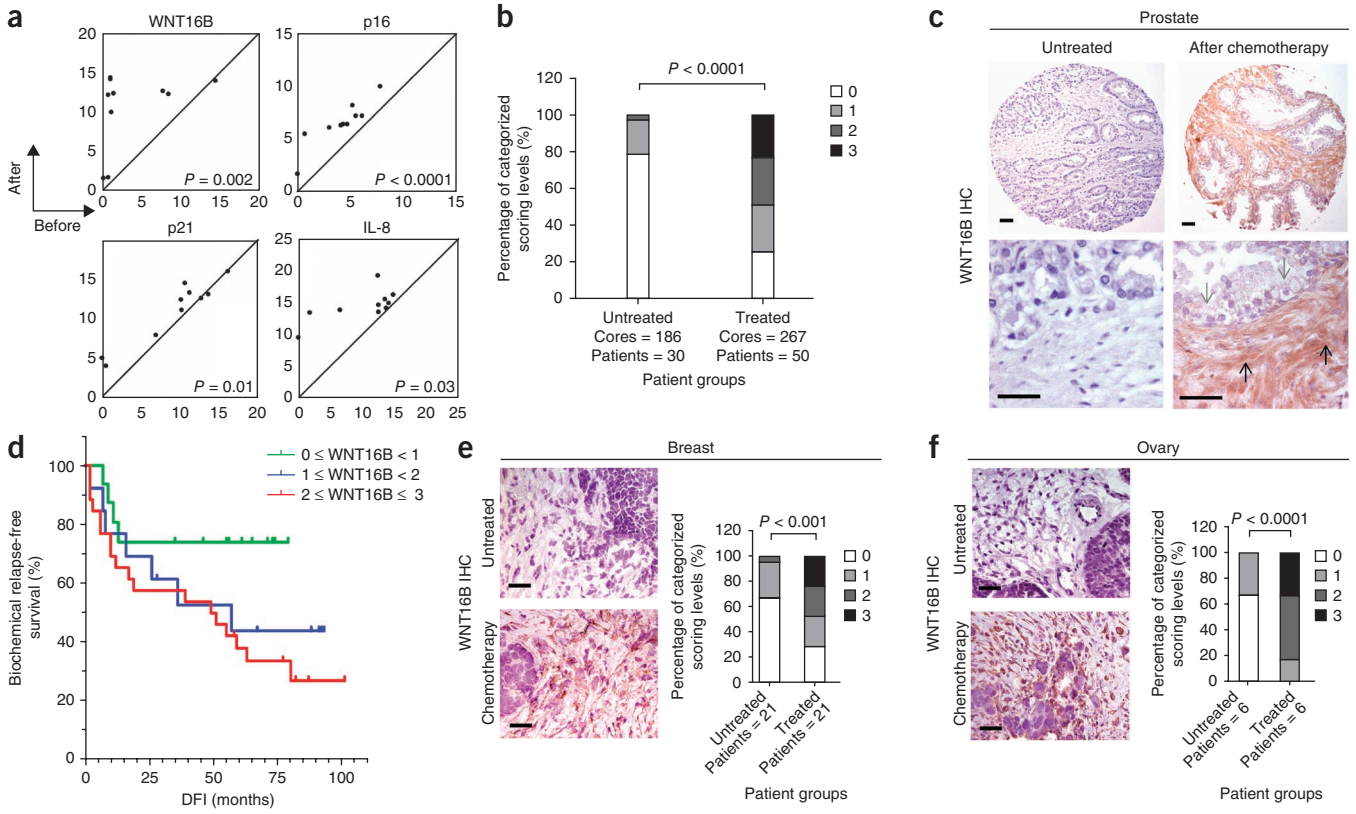

Figure 2 Cytotoxic chemotherapy induces WNT16B expression in the tumor microenvironment. (**a**) Chemotherapy-induced gene expression changes in human prostate-cancer–associated stroma measured by qRT-PCR of microdissected cells. The amounts of transcript before treatment (*x* axis) are plotted against the amounts of transcript after chemotherapy (*y* axis) from the same individual. Each data point represents the measurements from an individual patient. The results are shown as PCR cycle number relative to ribosomal protein L13 (RPL13), which served as the reference control. The *P* values were calculated by Student's *t* test. (**b**) IHC assessment of prostate stromal WNT16B expression in prostatectomy tissue samples from men with prostate cancer who were either untreated ($n = 30$) or treated with chemotherapy ($n = 50$). Patients were assigned to four categories based on their stromal WNT16B staining: 0, no expression; 1, faint or equivocal expression; 2, moderate expression; 3, intense reactivity. $P < 0.0001$ by ANOVA. (**c**) Representative example of intense WNT16B expression in prostate stroma after *in vivo* exposure to MIT and DOC. The black arrows denote areas of the stroma with fibroblasts and smooth muscle. Note the minimal WNT16B reactivity in the epithelium (gray arrows). Scale bars, 50 μm. (**d**) Kaplan-Meier plot of biochemical (prostate-specific antigen) relapse-free survival based on the expression of WNT16B in prostate stroma after exposure to MIT and DOC chemotherapy ($P = 0.04$ by log-rank test comparing WNT16B < 1 with WNT16B ≥ 2 survival distributions). DFI, disease-free interval from surgery. (**e**,**f**) WNT16B staining of breast (**e**) and ovarian (**f**) carcinoma from patients receiving neoadjuvant chemotherapy or no treatment before surgical resection. Staining is recorded on a 4-point scale: 0, no expression; 1, faint or equivocal expression; 2, moderate expression; 3, intense reactivity. Scale bars, 50 μm. The *P* values were calculated by ANOVA.

(PSC27^{WNT16B}) and fibroblast strains that expressed shRNAs specific to WNT16B (shRNA^{WNT16B}), which blocked the induction of WNT16B expression by RAD and MIT (**Supplementary Fig. 3a**,**b**). PSC27^{WNT16B}-conditioned medium significantly enhanced prostate cancer cell growth ($P < 0.01$) (**Fig. 3a**) and increased cellular migration and invasion ($P < 0.05$) compared to conditioned medium from PSC27 vector controls (PSC27^{C}) (**Fig. 3b** and **Supplementary Fig. 3c**,**d**), confirming that WNT16B can promote phenotypic changes in tumor cells through paracrine mechanisms.

The DDSP comprises a diverse spectrum of secreted proteins with the potential to alter the phenotypes of neighboring cells (**Fig. 1c**). We next sought to determine to what extent WNT16B is responsible for such effects in the context of the amalgam of factors induced by DNA damage. Conditioned medium from irradiated PSC27 fibroblasts (PSC27-RAD), representing the full DDSP, increased the proliferation (between 1.5-fold and twofold, $P < 0.05$) and invasiveness (between threefold and fourfold, $P < 0.05$) of neoplastic epithelial cells compared to conditioned medium from untreated PSC27 fibroblasts (**Fig. 3c**,**d**). Compared to irradiated PSC27 cells expressing control shRNAs, conditioned medium from PSC27-RAD + shRNA^{WNT16B} fibroblasts reduced these responses to the full DDSP by between 15% and 35%, depending on the cell line ($P < 0.05$) (**Fig. 3c**,**d**).

To investigate the *in vivo* consequences of WNT16B expression in the tumor microenvironment, we combined nontumorigenic BPH1 or tumorigenic PC3 cells with PSC27^{WNT16B} (BPH1+PSC27^{WNT16B} and PC3+PSC27^{WNT16B}, respectively) or control PSC27 (BPH1+PSC27^{C} and PC3+PSC27^{C}, respectively) fibroblasts and implanted the recombinants under the renal capsule of recipient mice (**Fig. 3e**). At 8 weeks after implantation, BPH1+PSC27^{WNT16B} grafts were larger than BPH1+PSC27^{C} grafts (~200 mm^3 compared to ~10 mm^3, respectively; $P < 0.001$) (**Supplementary Fig. 3e**). PC3+PSC27^{WNT16B} recombinants generated very large poorly differentiated and invasive tumors with an average size of 500 mm^3, which was substantially larger than any of the control tumors ($P < 0.001$) (**Fig. 3f** and **Supplementary Fig. 3f**).

In vivo, PC3 cells combined with PSC27-RAD cells expressing the full fibroblast DDSP resulted in substantially larger tumors

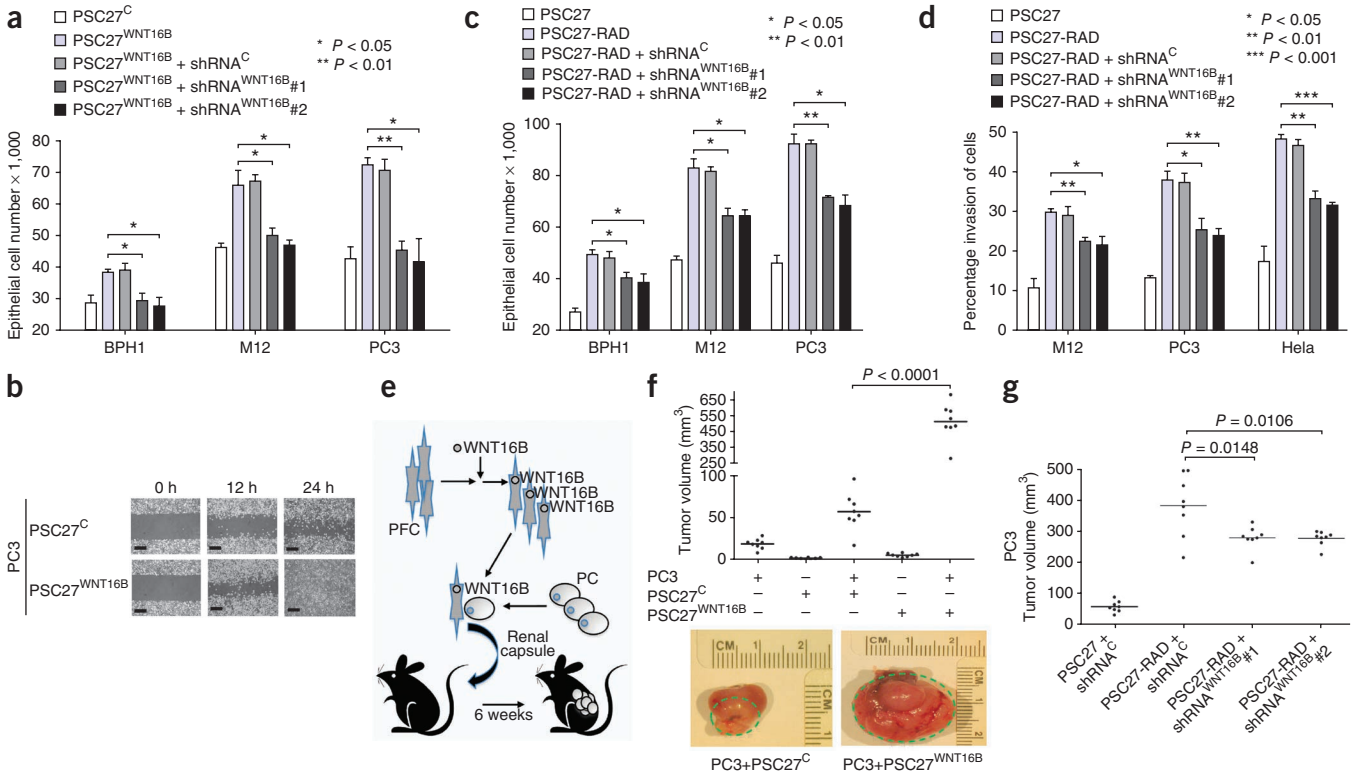

Figure 3 WNT16B is a major effector of the full DDSP and promotes the growth and invasion of prostate carcinoma. (**a**) Conditioned medium from WNT16B-expressing prostate fibroblasts (PSC27^{WNT16B}) promotes the proliferation of neoplastic prostate epithelial cells. shRNA^{C}, control shRNA; shRNA^{WNT16B}#1 and shRNA^{WNT16B}#2, WNT16B-specific shRNAs. (**b**) Scratch assay showing the enhanced motility of PC3 cells exposed to conditioned medium from prostate fibroblasts expressing a control vector (PSC27^{C}) or fibroblasts expressing WNT16B (PSC27^{WNT16B}). Scale bars, 100 μm. (**c**) The full fibroblast DDSP induced by radiation (PSC27-RAD) promotes the proliferation of tumorigenic prostate epithelial cells. The proliferative effect is significantly attenuated by the suppression of damage-induced expression of WNT16B (PSC27-RAD+shRNA^{WNT16B}). (**d**) The full paracrine-acting fibroblast DDSP induced by radiation (PSC27-RAD) promotes the invasion of neoplastic epithelial cells. Invasion is significantly attenuated by the suppression of damage-induced expression of WNT16B (PSC27-RAD+shRNA^{WNT16B}). Data in **a**, **c** and **d** are mean ± s.e.m. of triplicates, with *P* values calculated by ANOVA followed by *t* test. (**e**) Schematic of the xenograft cell recombination experiment to assess the ability of fibroblasts expressing WNT16B to influence prostate tumorigenesis *in vivo*. PFC, prostate fibroblast cells; PC, prostate cancer cells. (**f**) Prostate fibroblasts engineered to express WNT16B promote the growth of prostate carcinoma *in vivo*. Subrenal capsule grafts comprised of PC3 prostate epithelial cells alone, PC3 cells in combination with PSC27^{C} control fibroblasts or PC3 cells in combination with PSC27^{WNT16B} fibroblasts are shown. The green dashed lines denote the size of the tumor outgrowth from the kidney capsule. (**g**) Irradiated prostate fibroblasts (PSC27-RAD) promote the growth of prostate carcinoma cells *in vivo*, and this effect is significantly attenuated by the suppression of fibroblast WNT16B using WNT16B-specific shRNAs (PSC27-RAD+shRNA^{WNT16B}) ($P < 0.05$). Shown are tumor volumes 8 weeks after renal capsule implantation of PC3 and PSC27 cell grafts. In **f** and **g**, horizontal lines denote the mean of each group of eight tumors, and *P* values were determined by ANOVA followed by *t* test.

than PC3 cells combined with untreated PSC27 control fibroblasts ($P < 0.001$) (**Fig. 3g**). Reducing the fibroblast contribution of WNT16B attenuated the PSC27-RAD effects: grafts of PC3+PSC27-RAD averaged 380 mm^3, whereas PC3 cells combined with PSC27-RAD+shRNA^{WNT16B} averaged 280 mm^3, a ~25% reduction in tumor size when fibroblast WNT16B was suppressed ($P < 0.02$) (**Fig. 3g**). Taken together, these findings show that paracrine WNT16B activity can promote tumor growth *in vivo* and accounts for a substantial component of the full DDSP effect on neoplastic epithelium.

WNT16B signals through β-catenin and induces an EMT

Having established that WNT16B can promote tumor growth through paracrine signaling, we next sought to determine the mechanism(s) by which it does so. PSC27^{WNT16B}-conditioned medium activated

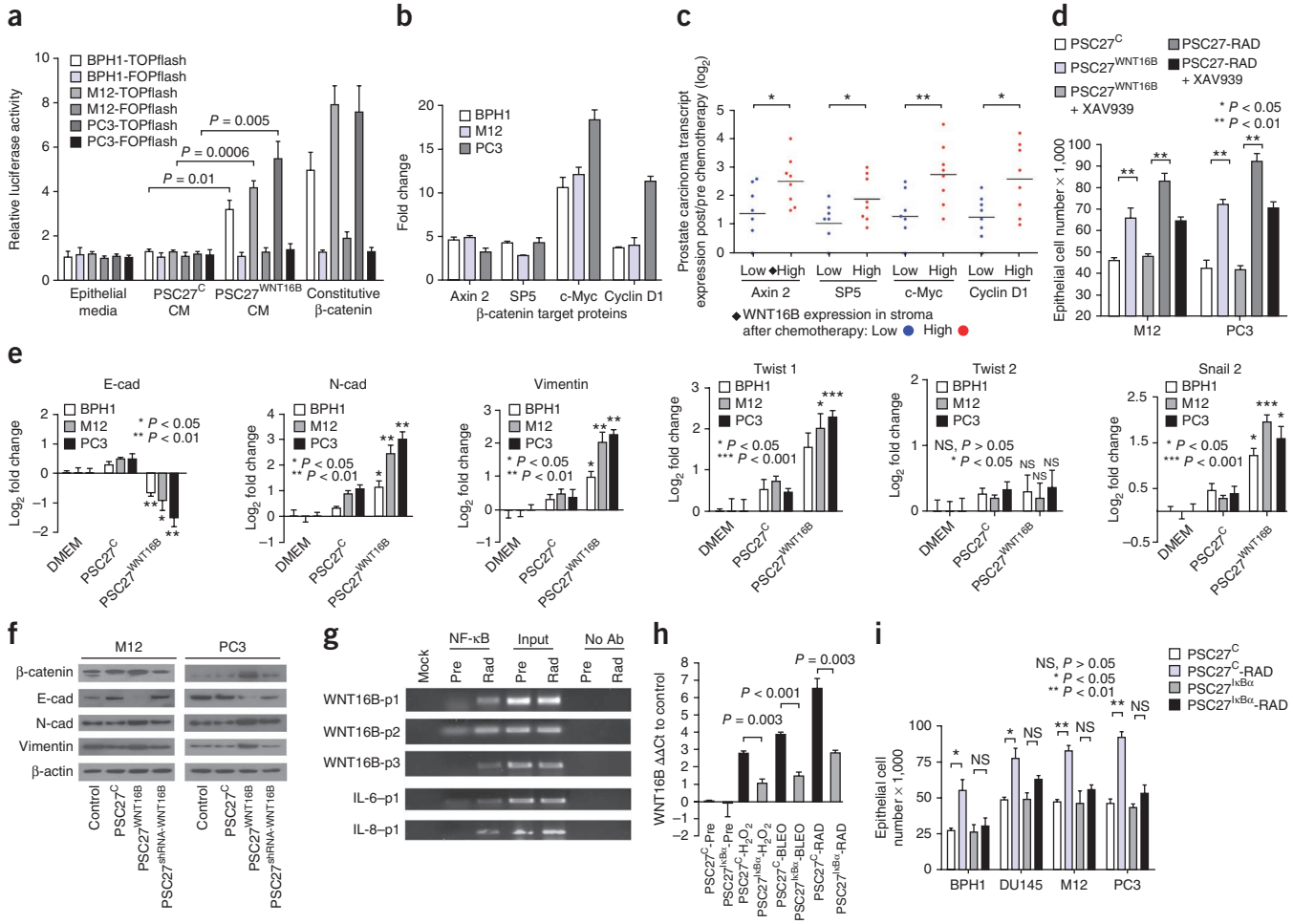

Figure 4 Genotoxic stress upregulates WNT16B through NF-κB and signals through the canonical Wnt–β-catenin pathway to promote tumor cell proliferation and the acquisition of mesenchymal characteristics. (**a**) Assay of canonical Wnt pathway signaling through activation of a TCF/LEF luciferase reporter construct (TOPflash) or a control reporter (FOPflash). Epithelial cells were exposed to conditioned medium (CM) from PSC27 prostate fibroblasts expressing WNT16B (PSC27^{WNT16B}) or control vector (PSC27^{C}). Data are mean ± s.e.m. of triplicates, and *P* values were determined by ANOVA followed by *t* test. (**b**) qRT-PCR assessment of the expression of β-catenin target genes in prostate cancer cell lines (BPH1, M12 and PC3) before and 72 h after exposure to PSC27^{WNT16B}–conditioned medium. Data represent the mean ± s.e.m. fold change after as compared to before exposure for three replicates. (**c**) Expression of β-catenin target genes in human prostate cancers *in vivo* after neoadjuvant treatment with MIT and DOC. Log2 transcript amounts in carcinoma cells after and before chemotherapy are shown in relation to low (blue) or high (red) WNT16B expression in the prostate stroma. Each data point represents an individual patient; $n = 8$ patients. Horizontal bars are group means. $^{*}P < 0.05$, $^{**}P < 0.01$ by ANOVA followed by *t* test. (**d**) The β-catenin pathway inhibitor XAV939 suppresses the proliferation of prostate cancer cells in response to PSC27^{WNT16B} CM and attenuates the response to the full DDSP in PSC27-RAD–conditioned medium. Cell numbers were determined 72 h after treatment. (**e**) Quantification of transcripts in neoplastic prostate epithelial cells encoding proteins associated with a phenotype of EMT. Measurements are from epithelial cells exposed to control media (DMEM), media conditioned by PSC27 fibroblasts (PSC27^{C}) or PSC27 fibroblasts expressing WNT16B (PSC27^{WNT16B}). E-cad, E-cadherin; N-cad, N-cadherin. (**f**) Analysis of EMT-associated protein expression by western blot. M12 or PC3 cells were exposed to control media, media conditioned by PSC27 fibroblasts (PSC27^{C}), PSC27 fibroblasts expressing WNT16B (PSC27^{WNT16B}) or PSC27 fibroblasts expressing WNT16B and shRNA targeting WNT16B (PSC27$^{shRNA\text{-}WNT16B}$). (**g**) Chromatin immunoprecipitation assays identified NF-κB binding sites within the proximal promoter of the WNT16 gene. PCR reaction products from Mock (no DNA loading), NF-κB immunoprecipitation, input control DNA and no antibody (Ab) control before treatment (Pre) and after irradiation (Rad). p1, p2 and p3 indicate primer pairs corresponding to putative NF-κB binding regions in WNT16, IL-6 and IL-8, respectively (see the **Supplementary Methods** for the primer sequences). (**h**) Analysis of WNT16B transcript expression by qRT-PCR in PSC27 prostate fibroblasts with (PSC27^{IκBα}) or without (PSC27^{C}) inhibition of NF-κB signaling before and after DNA-damaging exposures. (**i**) Inhibition of NF-κB signaling in fibroblasts responding to DNA damage attenuates the effect of the DDSP on tumor cell proliferation. Cell numbers were determined 72 h after RAD exposure to conditioned medium from fibroblasts with (PSC27^{IκBα}) or without (PSC27^{C}) inhibition of NF-κB signaling. Data in **d**, **e**, **h** and **i** are mean ± s.e.m. of triplicates, and *P* values were determined by ANOVA followed by *t* test.

canonical Wnt signaling in BPH1, PC3 and M12 prostate cancer cells, as measured by assays of β-catenin–mediated transcription through T cell factor/lymphoid enhancer binding factor (TCF/LEF) binding sites (**Fig. 4a**). Known β-catenin target genes, including *AXIN2* and *MYC*, were upregulated (approximately fivefold and over tenfold, respectively) after exposure to WNT16B-enriched conditioned medium (**Fig. 4b**). In human prostate cancers treated with chemotherapy, β-catenin localized in the nucleus of tumor cells (**Supplementary Fig. 4a**). We also found that β-catenin target genes were expressed more highly in tumors with elevated stromal WNT16B expression relative to those with low WNT16B expression ($P < 0.05$) (**Fig. 4c**). To confirm that β-catenin signaling contributed to the epithelial phenotypes resulting from exposure to PSC27-RAD–conditioned medium, we treated prostate cancer cells with the tankyrase inhibitor XAV939, which stabilizes axin and inhibits β-catenin–mediated transcription[24]. XAV939 completely suppressed the proliferative and invasive responses induced by WNT16B and markedly attenuated the effects of the PSC27-RAD DDSP (**Fig. 4d** and **Supplementary Fig. 4b**).

Wnt signaling is known to promote the acquisition of mesenchymal cell characteristics that can influence the migratory and invasive behavior of epithelial cells through an EMT[25–27]. Loss of CDH1 (also known as E-cadherin), the prototypic epithelial adhesion molecule in adherens junctions, and gain of CDH2 (also known as N-cadherin) expression are among the main hallmarks of an EMT[28,29]. After exposure of PC3 cells to PSC27^{WNT16B}-conditioned medium, the number of E-cadherin transcripts decreased 64%, whereas the number of N-cadherin transcripts increased fourfold ($P < 0.05$). Similar alterations occurred in M12 and BPH1 cells (**Fig. 4e**,**f**). Inhibiting β-catenin pathway signaling with XAV939 in epithelial cells blocked the WNT16B-induced EMT-associated gene expression (**Supplementary Fig. 4c**). Exposure to PSC27^{WNT16B}-conditioned medium also promoted mesenchymal characteristics in MDA-MD-231 breast cancer and SKOV3 ovarian cancer cells (**Supplementary Fig. 4d**).

Genotoxic stress induces WNT16B expression through NF-κB

A key pathway linking DNA damage with apoptosis, senescence and DNA repair mechanisms involves activating the NF-κB complex[30,31]. NF-κB is also pivotal in mediating the stress-associated induction of inflammatory networks, including the upregulation and secretion of interkeukin-6 (IL-6) and IL-8 (refs. 23,32). We therefore sought to determine whether DNA-damage–induced WNT16B expression is mediated by NF-κB. We identified NF-κB binding motifs in the WNT16B promoter region and confirmed their function using *WNT16B* promoter constructs. Compared to untreated cells, both RAD and tumor necrosis factor α (TNF-α), which are known NF-κB activators, induced WNT16B reporter activity ($P < 0.01$) (**Fig. 4g** and **Supplementary Fig. 5a–d**). We next generated PSC27 prostate fibroblasts with stable expression of a mutant nuclear factor of κ light polypeptide gene enhancer in B cells inhibitor, α (IκBα) (PSC27^{IκBα}),

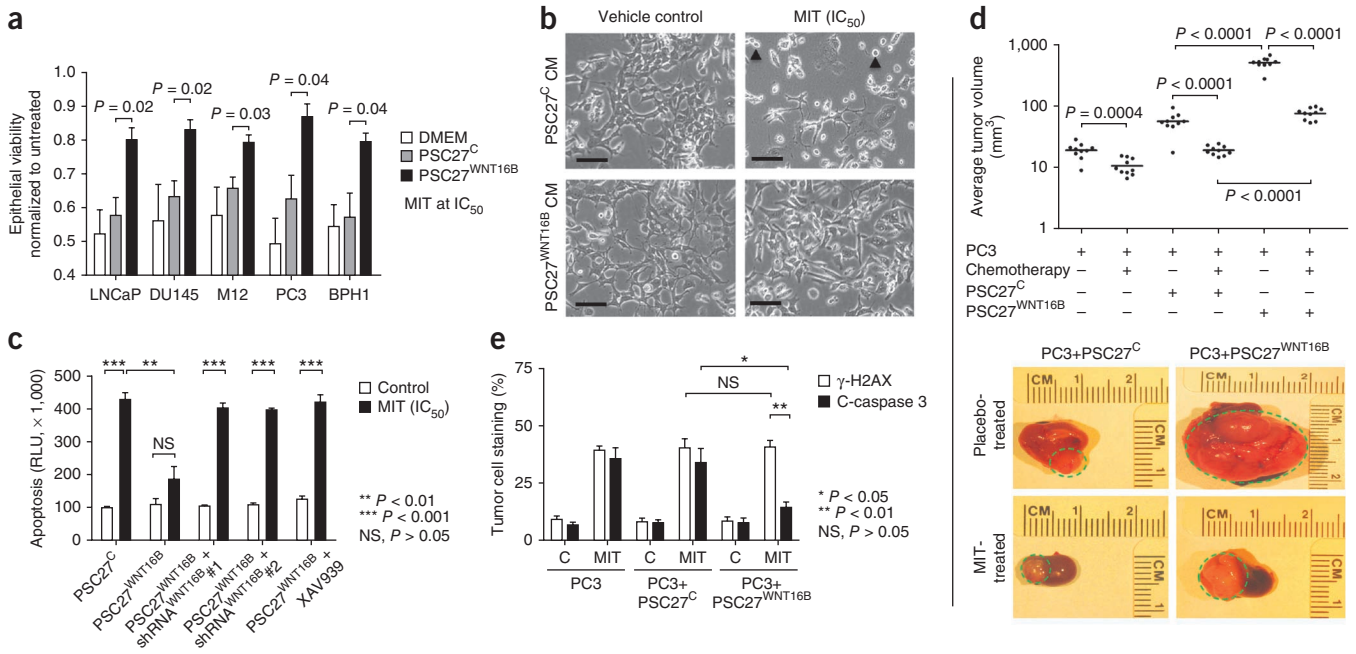

Figure 5 Paracrine-acting WNT16B promotes the resistance of prostate carcinoma to cytotoxic chemotherapy. (**a**) Viability of prostate cancer cells 3 d after treatment with a half-maximal inhibitory concentration (IC_{50}) of MIT and medium conditioned by fibroblasts with (PSC27^{WNT16B}) or without (PSC27^{C}) WNT16B. (**b**) Bright field microscopic view of PC3 cells cultured with control or PSC27^{WNT16B}-conditioned medium photographed 24 h after exposure to vehicle or the IC_{50} of MIT. Arrowheads denote apoptotic cell bodies. Scale bars, 50 μm. (**c**) Acute tumor cell responses to chemotherapy *in vitro*. Quantification of apoptosis by assays reflecting combined caspase 3 and 7 activity measured 24 h after the exposure of PC3 cells to vehicle or the IC_{50} of MIT. Data in **a** and **c** are mean ± s.e.m. of triplicate experiments, and *P* values were determined by ANOVA followed by *t* test. RLU, relative luciferase unit. (**d**) *In vivo* responses of PC3 tumors to MIT chemotherapy. Grafts were comprised of PC3 cells alone or PC3 cells combined with either PSC27 prostate fibroblasts expressing a control vector (PC3+PSC27^{C}) or PSC27 prostate fibroblasts expressing WNT16B (PC3+PSC27^{WNT16B}). MIT was administered every 2 weeks for three cycles, and grafts were harvested and tumor volumes determined 1 week after the final MIT treatment. Each data point represents an individual xenograft. Horizontal lines are group means of ten tumors, with *P* values determined by ANOVA followed by *t* test. (**e**) Acute tumor cell responses to chemotherapy *in vivo*. Quantification of apoptosis by cleaved caspase 3 (C-caspase 3) IHC and of DNA damage by γ-H2AX immunofluorescence in PC3 and fibroblast xenografts measured 24 h after *in vivo* treatment with vehicle (C) or MIT. Values represent a minimum of 100 cells counted from each of 3–5 tumors per group. Data are mean ± s.e.m., and *P* values were determined by ANOVA followed by *t* test.

which prevents IκB kinase (IKK)-dependent degradation of IκBα and thus attenuates NF-κB signaling. After irradiation of PSC27 cells, NF-κB translocated to the nucleus and induced NF-κB reporter activity >100-fold (**Supplementary Fig. 5d**,**e**). In comparison, the amount of nuclear NF-κB in PSC27^{IκBα}-RAD cells was markedly lower. The PSC27^{IκBα} cells with impaired NF-κB activation had a significant attenuation of induction of *WNT16B* expression after treatment with H_2O_2, BLEO or RAD ($P < 0.05$) (**Fig. 4h**).

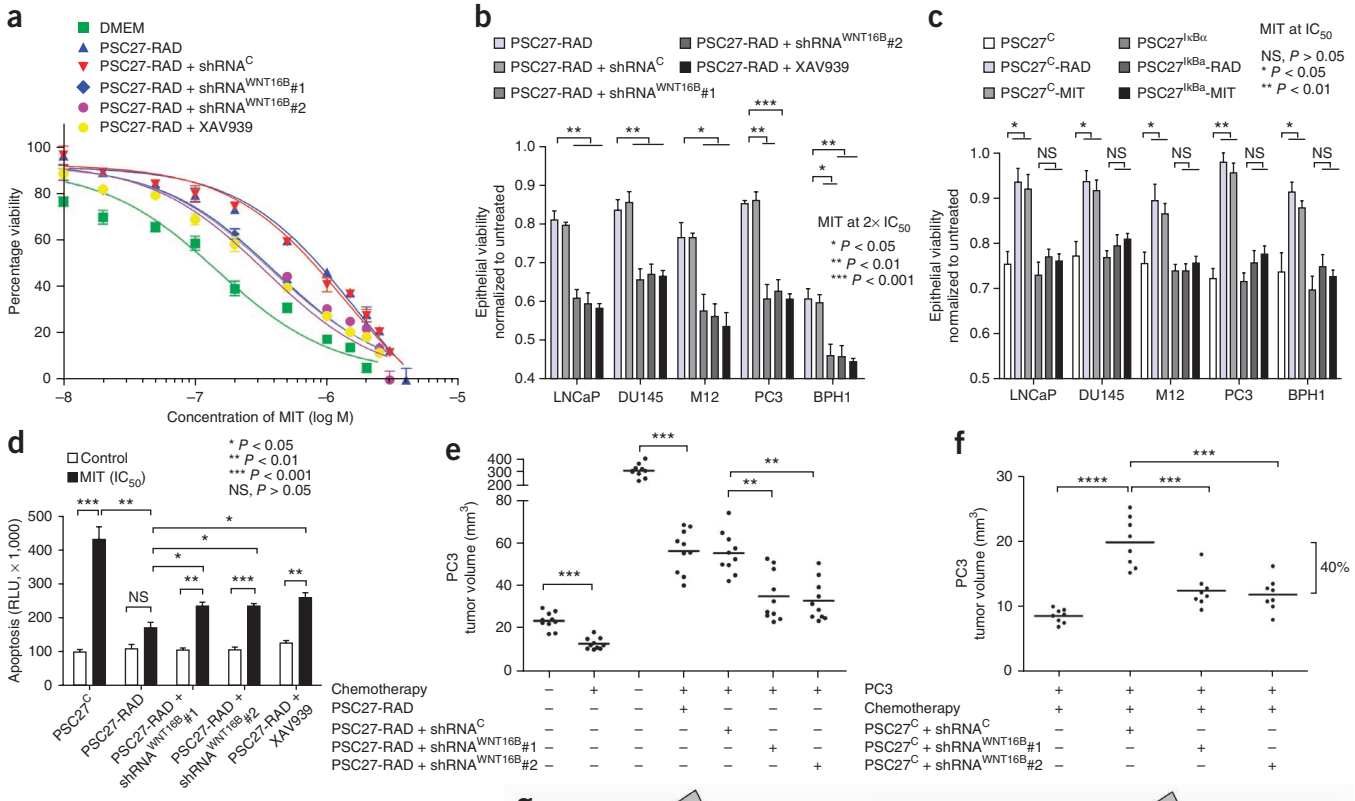

Figure 6 Chemotherapy resistance promoted by damaged fibroblasts is attenuated by blocking WNT16B, β-catenin or NF-κB signaling. (**a**) Viability of prostate cancer cells across a range of MIT concentrations with (PSC27-RAD+shRNA^{WNT16B}) or without (PSC27-RAD+shRNA^{C}) the suppression of WNT16B in irradiated-fibroblast–conditioned medium or with the addition of the β-catenin pathway inhibitor XAV939. Data are mean ± s.e.m. of triplicates. (**b**) Viability of prostate cancer cells 3 d after treatment with two times the IC_{50} of MIT in the context of conditioned medium from irradiated prostate fibroblasts (PSC27-RAD) expressing shRNAs targeting and suppressing WNT16B (shRNA^{WNT16B}), a vector control (shRNA^{C}) or combined with the β-catenin pathway inhibitor XAV939. (**c**) Viability of prostate cancer cells 3 d after treatment with the IC_{50} of MIT in the context of conditioned medium from prostate fibroblasts pretreated with radiation (PSC27-RAD) or MIT (PSC27-MIT) and with (PSC27^{IκBα}) or without (PSC27^{C}) the suppression of NF-κB signaling. (**d**) Acute tumor cell responses to chemotherapy *in vitro*. Quantification of apoptosis by caspase 3 and 7 activity measured 24 h after the exposure of PC3 cells to vehicle or the IC_{50} of MIT. Data for **b**, **c** and **d** are mean ± s.e.m. of triplicates, and *P* values were determined by ANOVA followed by *t* test. (**e**,**f**) *In vivo* effects of MIT chemotherapy in the context of suppressing the induction of the expression of fibroblast WNT16B. Tumors comprised PC3 cells in combination with irradiated (PSC27-RAD) fibroblasts (**e**) or unirradiated (PSC27^{C}) (**f**) prostate fibroblasts expressing shRNAs targeting WNT16B (shRNA^{WNT16B}) or a vector control (shRNA^{C}). MIT was administered every 2 weeks for three cycles, and grafts were harvested and tumor volumes determined 1 week after the final treatment. Each data point represents an individual xenograft. Tumor volumes of PSC27^{C}+shRNA^{C} grafts in **f** averaged 20 mm^3, and tumor volumes of PSC27^{C}+shRNA^{WNT16B} grafts averaged 12 mm^3 ($P < 0.001$). Horizontal lines are group means, with $n = 10$ in **e** and $n = 8$ in **f**. *P* values were determined by ANOVA followed by *t* test. The bracket boundaries in **f** are the group means for PSC27^{C}+shRNA^{C} grafts compared to PSC27^{C}+shRNA^{WNT16B} grafts showing a 40% difference in size. Asterisks, as for the previous panel. (**g**) Model for cell nonautonomous therapy-resistance effects originating in the tumor microenvironment in response to genotoxic cancer therapeutics. The initial round of therapy engages an apoptotic or senescence response in subsets of tumor cells and activates a DNA damage response (DDR) in DDR-competent benign cells (+DDR) comprising the tumor microenvironment. The DDR includes a spectrum of autocrine- and paracrine-acting proteins that are capable of reinforcing a senescent phenotype in benign cells and promoting tumor repopulation through progrowth signaling pathways in neoplastic cells. Paracrine-acting secretory components such as WNT16B also promote resistance to subsequent cycles of cytotoxic therapy. CEC, cancer epithelial cell; BEC, benign epithelial cell; FC, fibroblast cell; –DDR, DDR-incompetent benign cells.

We next determined whether suppressing fibroblast NF-κB signaling in response to DNA damage would attenuate the pro-proliferative effects of the PSC27-RAD DDSP. Whereas PSC27-RAD–conditioned medium promoted prostate epithelial cell proliferation, conditioned medium from PSC27^{IκBα}-RAD cells failed to do so (**Fig. 4i**). These experiments identify *WNT16B* as a new member of the cellular genomic program that is regulated by NF-κB signaling in response to DNA damage.

Paracrine WNT16B attenuates the effect of cytotoxic therapy

The preceding experiments suggested that in addition to tumor-promoting effects, paracrine-acting WNT16B may influence the responses of tumors to genotoxic cancer therapeutics. To evaluate this possibility, we studied MIT, a type 2 topoisomerase inhibitor that produces DNA strand breaks, leading to growth arrest, senescence or apoptosis, which is in clinical use for the treatment of advanced prostate cancer. Prostate cancer cells exposed to PSC27^{WNT16B}-conditioned medium compared to control medium consistently showed significant attenuation of chemotherapy-induced cytotoxicity across a range of MIT concentrations after 3 d ($P < 0.05$) (**Fig. 5a** and **Supplementary Fig. 6a**). Short-term cell viability assays confirmed that, compared to controls, PSC27^{WNT16B}-conditioned medium improved cancer cell survival after acute 12-h exposures to MIT ($P < 0.01$) (**Supplementary Fig. 6b**). Apoptotic responses measured after 24 h of MIT exposure were substantially attenuated by PSC27^{WNT16B}-conditioned medium ($P < 0.01$), an effect that was blocked by treatment with XAV939 (**Fig. 5b**,**c**). To determine whether these observations were of relevance to tumor therapy *in vivo*, we treated mice with tumor grafts comprised of PC3 cells plus PSC27^{WNT16B} or PSC27^{C} fibroblasts with three cycles of MIT given every other week. MIT treatment significantly reduced the tumor volumes ($P < 0.001$). However, grafts of tumor cells with PSC27^{WNT16B} fibroblasts attenuated the tumor inhibitory effects of MIT compared to tumor cells grafted with control PSC27 fibroblasts: PC3+PSC27^{C} and PC3+PSC27^{WNT16B} tumors averaged 13 mm^3 and 78 mm^3, respectively ($P < 0.001$) (**Fig. 5d**). Experiments using MDA-MB-231 breast cancer cells plus breast fibroblasts produced similar results (**Supplementary Fig. 6c**). To evaluate the influence of WNT16B on the acute effects of chemotherapy, we examined cohorts of PC3+PSC27^{C} and PC3+PSC27^{WNT16B} xenografts 24 h after MIT treatment to quantify DNA damage using γ-H2AX immunofluorescence and apoptosis using cleaved caspase 3 immunohistochemistry (IHC). Compared to PC3+PSC27^{C} grafts, there was no difference in the number of DNA damage foci in PC3+PSC27^{WNT16B} tumors, but significantly fewer apoptotic cells were present (34% compared to 14%, respectively; $P < 0.05$) (**Fig. 5e**).

The conditioned medium from PSC27-RAD cells, representing the full fibroblast DDSP, significantly increased the viability of PC3 cancer cells exposed to MIT concentrations ranging between 0.1–1 μM *in vitro* ($P < 0.01$) (**Fig. 6a**). In comparison to PSC27-RAD–conditioned medium, PSC27-RAD+shRNA^{WNT16B} or PSC27^{IκBα}RAD fibroblasts, engineered to suppress WNT16B expression or NF-κB activation, respectively, substantially augmented the effects of MIT, further increasing apoptosis and reducing tumor cell viability by 30–40%. Blocking β-catenin signaling in carcinoma cells with XAV939 also attenuated the effects of PSC27-RAD–conditioned medium on promoting tumor cell survival (**Fig. 6b–d** and **Supplementary Fig. 7a**,**b**). This effect of WNT16B was also evident *in vivo*. PC3+PSC27-RAD tumor grafts averaged 300 mm^3 in size compared to 25 mm^3 for grafts of PC3 cells alone ($P < 0.001$). MIT chemotherapy suppressed the growth of the PC3+PSC27-RAD grafts, though residual tumors were still readily detectable and averaged 55 mm^3 in size (**Fig. 6e**). However, after MIT treatment, residual tumors of PC3 cells with PSC27-RAD + shRNA^{WNT16B} fibroblasts, with attenuated WNT16B induction, were on average ~33% smaller than PC3+PSC27-RAD tumors ($P < 0.001$) (**Fig. 6e**). Experiments with MDA-MD-231 cells and breast fibroblasts produced similar results (**Supplementary Fig. 7c**). To more accurately mimic the clinical situation of cancer therapy, we also grafted tumor cells with unirradiated PSC27 fibroblasts (PSC27^{C}) and followed the same treatment schema of three MIT cycles. Tumors from mice treated with MIT were substantially smaller than tumors from untreated mice ($P < 0.001$). Attenuating the induction of WNT16B further enhanced the effects of chemotherapy: after MIT treatment, grafts of PC3 cells and PSC27^{C} + shRNA^{WNT16B} were on average 40% smaller than grafts of PC3 cells combined with PSC27^{C} cells without shRNA^{WNT16B} ($P < 0.001$) (**Fig. 6f** and **Supplementary Fig. 7d**).

DISCUSSION

Optimizing radiotherapy and chemotherapy for the treatment of malignant neoplasms has relied on the iterative development and testing of models involving tumor growth dynamics, mutation rates and cell-kill kinetics. However, the most theoretically effective tumoricidal strategies must usually be tempered because of detrimental effects to the host. This reality has led to the development of regimens in which therapies are administered at intervals or cycles to avoid irreparable damage to vital host functions. However, the recovery and repopulation of tumor cells between treatment cycles is a major cause of treatment failure[15,16]. Interestingly, rates of tumor cell repopulation have been shown to accelerate in the intervals between successive courses of treatment, and solid tumors commonly show initial responses followed by rapid regrowth and subsequent resistance to further chemotherapy. Our results indicate that damage responses in benign cells comprising the tumor microenvironment may directly contribute to enhanced tumor growth kinetics (**Fig. 6g**).

The autocrine- and paracrine-acting influences of genotoxic stress responses can exert complex and potentially conflicting cell non-autonomous effects[33,34]. Overall, our findings are in agreement with studies of DNA damage in which the execution of a signaling program culminating in a senescence phenotype is accompanied by elevated concentrations of specific extracellular proteins termed a 'senescence messaging secretome' or a 'senescence-associated secretory phenotype'[33,34]. DNA damage responses and senescence programs can clearly operate in a cell autonomous 'intrinsic' manner to arrest cell growth and inhibit tumor progression, as has been observed in premalignant nevi[35]. Secreted factors such as insulin-like growth factor binding protein 7 (IGFBP7) and the chemokine (C-X-C motif) receptor 2 (CXCR2) ligands IL-6 and IL-8 participate in a positive feedback loop to fortify the senescence growth arrest induced by oncogenic stress and also promote immune responses that clear senescent cells and enhance tumor regression[23,32,36,37]. However, in addition to proinflammatory cytokines, the damage response program comprises proteases and mitogenic growth factors, such as MMPs, hepatocyte growth factor (HGF), vascular endothelial growth factor (VEGF) and epidermal growth factor receptor (EGFR) ligands that have clear roles in promoting tumor growth, inhibiting cellular differentiation, enhancing angiogenesis and influencing treatment resistance[19,20,38]. This concept is supported by reports of tissue-specific chemoresistant survival niches involving hematopoietic neoplasms, such as lymphomas[39]. The situation also has parallels with studies of radiation and chemotherapy paradoxically promoting tumor dissemination[40].

Collectively, these studies support several conclusions: first, the outcomes of genotoxic exposures to any specific benign or neoplastic cell depend on the integration of innate damage response capabilities and the context that is dictated by the composition of the tumor microenvironment; second, although intrinsic drug resistance is clearly operative in some cancers, acquired resistance can also occur without alterations in intrinsic cellular chemosensitivity[41], and our results provide strong support for previous studies that implicate constituents of the tumor microenvironment as important contributors to this resistance[42–44]; and third, specific microenvironment DDSP proteins that promote therapy resistance such as WNT16B are attractive targets for augmenting responses to more general genotoxic therapeutics. However, the complexity of the damage response program also supports strategies that are focused on inhibiting upstream master regulators, such as NF-κB[45], that may be more efficient and effective adjuncts to cytotoxic therapies, provided their side effects are tolerable.

METHODS

Methods and any associated references are available in the online version of the paper.

Accession codes. Microarray data are deposited in the Gene Expression Omnibus database with accession code GSE26143.

Note: Supplementary information is available in the online version of the paper.

ACKNOWLEDGMENTS

We thank J. Dean and D. Bianchi-Frias for helpful comments, A. Moreno for administrative assistance and N. Clegg for bioinformatics support. S. Hayward, Vanderbilt University, and J. Ware, Medical College of Virginia, provided BPH1 and M12 cells, respectively. Primary human prostate (PSC27), ovarian (OVF28901) and breast (HBF1203) fibroblasts were provided by B. Knudsen, Cedars Sinai Medical Center, E. Swisher, University of Washington, and P. Porter through the Seattle Breast SPORE (P50 CA138293), Fred Hutchinson Cancer Research Center, respectively. B. Torok-Strorb, Fred Hutchinson Cancer Research Center, provided HS5 and HS27A HPV E6/E7 immortalized human bone marrow stromal cells. We thank the clinicians who participated in the trials of neoadjuvant chemotherapy: M. Garzotto, T. Takayama, P. Lange, W. Ellis, S. Lieberman and B.A. Lowe. We are also grateful for the participation of the patients and their families in these studies. Breast cancer specimens were obtained from the Fred Hutchinson Cancer Research Center/University of Washington Medical Center Breast Specimen Repository. We thank N. Urban, Fred Hutchinson Cancer Research Center, for providing ovarian cancer biospecimens funded through the POCRC SPORE grant P50CA83636. This work was supported by a fellowship from the Department of Defense (PC073217), R01CA119125, the National Cancer Institute Tumor Microenvironment Network U54126540, the Pacific Northwest Prostate Cancer SPORE P50CA097186 and the Prostate Cancer Foundation.

AUTHOR CONTRIBUTIONS

Y.S. designed and conducted experiments, and wrote the manuscript. J.C. provided reagents and technical advice. C.H., T.M.B. and P.P. provided clinical materials for the assessments of treatment responses. I.C. analyzed data. L.T. analyzed tissue histology and immunohistochemical assays. P.S.N. designed experiments, analyzed data and wrote the manuscript.

COMPETING FINANCIAL INTERESTS

The authors declare no competing financial interests.

Published online at http://www.nature.com/doifinder/10.1038/nm.2890.
Reprints and permissions information is available online at http://www.nature.com/reprints/index.html.

1. Longley, D.B. & Johnston, P.G. Molecular mechanisms of drug resistance. *J. Pathol.* **205**, 275–292 (2005).
2. Wang, T.L. *et al.* Digital karyotyping identifies thymidylate synthase amplification as a mechanism of resistance to 5-fluorouracil in metastatic colorectal cancer patients. *Proc. Natl. Acad. Sci. USA* **101**, 3089–3094 (2004).
3. Schmitt, C.A., Rosenthal, C.T. & Lowe, S.W. Genetic analysis of chemoresistance in primary murine lymphomas. *Nat. Med.* **6**, 1029–1035 (2000).
4. Helmrich, A. *et al.* Recurrent chromosomal aberrations in INK4a/ARF defective primary lymphomas predict drug responses *in vivo*. *Oncogene* **24**, 4174–4182 (2005).
5. Redmond, K.M., Wilson, T.R., Johnston, P.G. & Longley, D.B. Resistance mechanisms to cancer chemotherapy. *Front. Biosci.* **13**, 5138–5154 (2008).
6. Wilson, T.R., Longley, D.B. & Johnston, P.G. Chemoresistance in solid tumours. *Ann. Oncol.* **17** (suppl. 10), x315–x324 (2006).
7. Lee, S. & Schmitt, C.A. Chemotherapy response and resistance. *Curr. Opin. Genet. Dev.* **13**, 90–96 (2003).
8. Sakai, W. *et al.* Secondary mutations as a mechanism of cisplatin resistance in BRCA2-mutated cancers. *Nature* **451**, 1116–1120 (2008).
9. Kobayashi, H. *et al.* Acquired multicellular-mediated resistance to alkylating agents in cancer. *Proc. Natl. Acad. Sci. USA* **90**, 3294–3298 (1993).
10. Waldman, T. *et al.* Cell-cycle arrest versus cell death in cancer therapy. *Nat. Med.* **3**, 1034–1036 (1997).
11. Samson, D.J., Seidenfeld, J., Ziegler, K. & Aronson, N. Chemotherapy sensitivity and resistance assays: a systematic review. *J. Clin. Oncol.* **22**, 3618–3630 (2004).
12. Croix, B.S. *et al.* Reversal by hyaluronidase of adhesion-dependent multicellular drug resistance in mammary carcinoma cells. *J. Natl. Cancer Inst.* **88**, 1285–1296 (1996).
13. Kerbel, R.S. Molecular and physiologic mechanisms of drug resistance in cancer: an overview. *Cancer Metastasis Rev.* **20**, 1–2 (2001).
14. Wang, F. *et al.* Phenotypic reversion or death of cancer cells by altering signaling pathways in three-dimensional contexts. *J. Natl. Cancer Inst.* **94**, 1494–1503 (2002).
15. Kim, J.J. & Tannock, I.F. Repopulation of cancer cells during therapy: an important cause of treatment failure. *Nat. Rev. Cancer* **5**, 516–525 (2005).
16. Trédan, O., Galmarini, C.M., Patel, K. & Tannock, I.F. Drug resistance and the solid tumor microenvironment. *J. Natl. Cancer Inst.* **99**, 1441–1454 (2007).
17. Garzotto, M., Myrthue, A., Higano, C.S. & Beer, T.M. Neoadjuvant mitoxantrone and docetaxel for high-risk localized prostate cancer. *Urol. Oncol.* **24**, 254–259 (2006).
18. Beer, T.M. *et al.* Phase I study of weekly mitoxantrone and docetaxel before prostatectomy in patients with high-risk localized prostate cancer. *Clin. Cancer Res.* **10**, 1306–1311 (2004).
19. Bavik, C. *et al.* The gene expression program of prostate fibroblast senescence modulates neoplastic epithelial cell proliferation through paracrine mechanisms. *Cancer Res.* **66**, 794–802 (2006).
20. Coppé, J.P. *et al.* Senescence-associated secretory phenotypes reveal cell-nonautonomous functions of oncogenic RAS and the p53 tumor suppressor. *PLoS Biol.* **6**, 2853–2868 (2008).
21. Clevers, H. Wnt/β-catenin signaling in development and disease. *Cell* **127**, 469–480 (2006).
22. Binet, R. *et al.* WNT16B is a new marker of cellular senescence that regulates p53 activity and the phosphoinositide 3-kinase/AKT pathway. *Cancer Res.* **69**, 9183–9191 (2009).
23. Acosta, J.C. *et al.* Chemokine signaling via the CXCR2 receptor reinforces senescence. *Cell* **133**, 1006–1018 (2008).
24. Huang, S.M. *et al.* Tankyrase inhibition stabilizes axin and antagonizes Wnt signalling. *Nature* **461**, 614–620 (2009).
25. Thiery, J.P., Acloque, H., Huang, R.Y. & Nieto, M.A. Epithelial-mesenchymal transitions in development and disease. *Cell* **139**, 871–890 (2009).
26. Yook, J.I. *et al.* A Wnt-Axin2–GSK3β cascade regulates Snail1 activity in breast cancer cells. *Nat. Cell Biol.* **8**, 1398–1406 (2006).
27. Vincan, E. & Barker, N. The upstream components of the Wnt signalling pathway in the dynamic EMT and MET associated with colorectal cancer progression. *Clin. Exp. Metastasis* **25**, 657–663 (2008).
28. Wu, K. & Bonavida, B. The activated NF-κB–Snail–RKIP circuitry in cancer regulates both the metastatic cascade and resistance to apoptosis by cytotoxic drugs. *Crit. Rev. Immunol.* **29**, 241–254 (2009).
29. Peinado, H., Olmeda, D. & Cano, A. Snail, Zeb and bHLH factors in tumour progression: an alliance against the epithelial phenotype? *Nat. Rev. Cancer* **7**, 415–428 (2007).
30. Bernard, D. *et al.* Involvement of Rel/nuclear factor-κB transcription factors in keratinocyte senescence. *Cancer Res.* **64**, 472–481 (2004).
31. Berchtold, C.M., Wu, Z.H., Huang, T.T. & Miyamoto, S. Calcium-dependent regulation of NEMO nuclear export in response to genotoxic stimuli. *Mol. Cell. Biol.* **27**, 497–509 (2007).
32. Kuilman, T. *et al.* Oncogene-induced senescence relayed by an interleukin-dependent inflammatory network. *Cell* **133**, 1019–1031 (2008).
33. Kuilman, T. & Peeper, D.S. Senescence-messaging secretome: SMS-ing cellular stress. *Nat. Rev. Cancer* **9**, 81–94 (2009).
34. Fumagalli, M. & d'Adda di Fagagna, F. SASPense and DDRama in cancer and ageing. *Nat. Cell Biol.* **11**, 921–923 (2009).
35. Michaloglou, C. *et al.* BRAFE600-associated senescence-like cell cycle arrest of human naevi. *Nature* **436**, 720–724 (2005).
36. Xue, W. *et al.* Senescence and tumour clearance is triggered by p53 restoration in murine liver carcinomas. *Nature* **445**, 656–660 (2007).
37. Wajapeyee, N., Serra, R.W., Zhu, X., Mahalingam, M. & Green, M.R. Oncogenic BRAF induces senescence and apoptosis through pathways mediated by the secreted protein IGFBP7. *Cell* **132**, 363–374 (2008).

38. Coppé, J.P., Kauser, K., Campisi, J. & Beausejour, C.M. Secretion of vascular endothelial growth factor by primary human fibroblasts at senescence. *J. Biol. Chem.* **281**, 29568–29574 (2006).
39. Gilbert, L.A. & Hemann, M.T. DNA damage–mediated induction of a chemoresistant niche. *Cell* **143**, 355–366 (2010).
40. Biswas, S. *et al.* Inhibition of TGF-β with neutralizing antibodies prevents radiation-induced acceleration of metastatic cancer progression. *J. Clin. Invest.* **117**, 1305–1313 (2007).
41. Davis, A.J. & Tannock, J.F. Repopulation of tumour cells between cycles of chemotherapy: a neglected factor. *Lancet Oncol.* **1**, 86–93 (2000).
42. Meads, M.B., Hazlehurst, L.A. & Dalton, W.S. The bone marrow microenvironment as a tumor sanctuary and contributor to drug resistance. *Clin. Cancer Res.* **14**, 2519–2526 (2008).
43. Shree, T. *et al.* Macrophages and cathepsin proteases blunt chemotherapeutic response in breast cancer. *Genes Dev.* **25**, 2465–2479 (2011).
44. DeNardo, D.G. *et al.* Leukocyte complexity predicts breast cancer survival and functionally regulates response to chemotherapy. *Cancer Discov.* **1**, 54–67 (2011).
45. Chien, Y. *et al.* Control of the senescence-associated secretory phenotype by NF-κB promotes senescence and enhances chemosensitivity. *Genes Dev.* **25**, 2125–2136 (2011).

ONLINE METHODS

Cell cultures and treatments. We obtained epithelial cell lines from the American Type Culture Collection and cultured them according to the recommended protocols. Fibroblasts were grown until they were 80% confluent and were then treated with 0.6 mM hydrogen peroxide (PSC27-H_2O_2), 10 μg ml^{-1} bleomycin (PSC27-BLEO), 1 μM mitoxantrone (PSC27-MIT) or ionizing radiation by a ^{137}Cesium source at 743 rad min^{-1} (PSC27-RAD). Additional details of the cell culture methods are provided in the **Supplementary Methods**.

Gene expression analysis. We extracted total RNA from PSC27 cells using the RNeasy kit (QIAGEN), converted mRNAs to complementary DNAs (cDNAs) and amplified the cDNAs for one round using the MessageAmp aRNA Kit (Ambion), followed by aminoallyl-UTP incorporation into a second-round of amplification of the RNA. Samples were labeled with fluorescence dyes and hybridized to 44K Whole Human Genome Expression Microarray slides in accordance with the manufacturer's instructions (Agilent Technologies). Additional assays of transcript abundance were performed by qRT-PCR (**Supplementary Methods**).

Immunohistochemistry. We used a mouse monoclonal antibody to WNT16B (product number 552595, clone F4-1582, BD Pharmingen) at a dilution of 1:16,000 to immunolocalize WNT16B protein using an indirect three-step avidin-biotin-peroxidase method according to the manufacturer's instructions (VECTASTAIN Elite ABC Kit, Vector Labs). The expression of WNT16B by epithelium or fibromuscular stromal cells in each tissue section was recorded on a 4-point scale as follows: 3 for intensely expressed, 2 for moderately expressed, 1 for faintly or equivocally expressed and 0 for no expression of WNT16B by any stromal cells. Additional details are provided in the **Supplementary Methods**.

Characterization of cell phenotypes. We assessed cell proliferation using the CellTiter 96 AQueous One Solution Cell Proliferation Assay (MTS), with signals being captured using a 96-well plate reader. Serum-starved cells for transwell migration and invasion assays were added to the top chambers of Cultrex 24-well Cell Migration Assay plates (8 μm pore size) coated with or without basement membrane extract prepared as 0.5× of stock solution. After 12 h or 24 h, migrating or invading cells in the bottom chambers were stained, and the plate absorbance was recorded. Chemoresistance assays were performed using epithelial cells cultured with either DMEM and low serum (0.5% FCS) (denoted here as 'DMEM') or conditioned medium generated from PSC27 cells expressing vector controls, WNT16B or shRNAs. Cells received mitoxantrone treatment for 12 h, 24 h or 72 h at concentrations near the IC_{50} of each individual cell line. The percentage of viable cells was calculated by comparing the results of each experiment to the results from vehicle-treated cells. Each assay was repeated a minimum of three times, with results reported as means ± s.e.m.

***In vivo* studies.** The Institutional Animal Care and Use Committee (IACUC) of Fred Hutchinson Cancer Research Center reviewed and approved the animal protocols and procedures, with surgeries carried out per the US National Institutes of Health Guide for laboratory animals. To prepare tissue recombinants, 250,000 fibroblasts (PSC27 series) and epithelial cells were mixed at a 1:1 ratio in collagen gels. ICR–severe combined immunodeficient (SCID) male mice, obtained from Taconic, Inc, were anesthetized with isoflurane, and an oblique incision (<1 cm) was made on the kidney capsule surface parallel and adjacent to the long axis of each kidney. Cells were injected under the capsule with a blunt 25-gauge needle and a glass Hamilton syringe. The kidney was returned to the retroperitoneal space, and the skin was closed with surgical staples. The growth of the xenografts was assessed at weekly intervals, and the mice were killed at 8 weeks after transplantation. Each xenograft arm comprised 5–8 mice per xenograft type, either of individual cells or combinations of fibroblasts and epithelial cells. Additional details are provided in the **Supplementary Methods**.

For the chemotherapy studies, mice received cell grafts as described above and were followed for 2 weeks to allow tumor take. Starting from the third week after grafting, mice received mitoxantrone at a dose of 0.2 mg per kg intraperitoneally on day 1 of week 3, week 5 and week 7 (ref. 46). In total, three 2-week cycles were given, after which the mice were killed and their kidneys were removed for tumor measurements and histological analysis. Each experimental arm comprised 5–8 mice per treatment cohort. Additional details are provided in the **Supplementary Methods**.

Statistical analyses. All *in vitro* experiments were repeated at least three times, and data are reported as means ± s.e.m. Differences among groups and treatments were determined by ANOVA followed by *t* tests. $P \leq 0.05$ was considered significant.

Additional methods. Detailed methodology is described in the **Supplementary Methods**.

46. Alderton, P.M., Gross, J. & Green, M.D. Comparative study of doxorubicin, mitoxantrone, and epirubicin in combination with ICRF-187 (ADR-529) in a chronic cardiotoxicity animal model. *Cancer Res.* **52**, 194–201 (1992).

Published OnlineFirst May 22, 2012; DOI: 10.1158/1078-0432.CCR-11-0768

Clinical Cancer Research

Molecular Pathways: Involving Microenvironment Damage Responses in Cancer Therapy Resistance

Yu Sun and Peter S. Nelson

Clin Cancer Res 2012;18:4019-4025. Published OnlineFirst May 22, 2012.

Published OnlineFirst May 22, 2012; DOI: 10.1158/1078-0432.CCR-11-0768

Molecular Pathways: Involving Microenvironment Damage Responses in Cancer Therapy Resistance

Yu Sun[1] and Peter S. Nelson[1,2]

Abstract

The armamentarium of therapeutics used to treat cancer patients relies heavily on ionizing radiation and chemotherapeutic drugs that severely damage DNA. Tumor cells' responses to such treatments are heavily influenced by their environment: Physical contacts with structural elements such as the extracellular matrix, associations with resident and transitory benign cells such as fibroblasts and leukocytes, and interactions with numerous soluble endocrine and paracrine-acting factors all modulate tumor-cell behavior. Of importance, this complex tumor microenvironment is not static and dynamically responds to a variety of stimuli. Here, we describe emerging data indicating that genotoxic cancer treatments activate highly conserved damage response programs in benign constituents of the tumor microenvironment. These damage signals, transmitted via master regulators such as NF-κB, culminate in a powerful and diverse secretory program that generates a proangiogenic, proinflammatory microenvironment. Constituents of this program include interleukin (IL)-6, IL-8, hepatocyte growth factor, amphiregulin, matrix metalloproteinases, and other factors that have been shown to promote adverse tumor-cell phenotypes, such as enhanced resistance to treatment and rapid tumor repopulation. A detailed understanding of these survival signals induced in the context of genotoxic stress provides a platform for developing combinatorial treatment strategies that take into account malignant cells, the tumor microenvironment, and the dynamics exerted by the treatment itself. *Clin Cancer Res; 18(15); 4019–25. ©2012 AACR.*

Background

Since the advent of modern cancer therapeutics that involve the administration of drugs and ionizing radiation to eradicate neoplastic cells, both *de novo* and acquired resistance have been recognized as major barriers to cures. Most cancer-directed therapeutics fall broadly into 3 classes that exploit differential vulnerabilities in malignant tumors relative to benign tissue counterparts. The most commonly deployed therapies inflict substantial damage to nuclear DNA or cell division machinery, resulting in genotoxic catastrophe or the engagement of damage response mechanisms that halt cell proliferation. However, the lack of specificity of these interventions limits doses to avoid collateral damage to normal tissues. A second category of cancer therapeutics has emerged through a detailed understanding of oncogenic pathways that direct targeted inhibition of key drivers such as kinases, growth factors, and growth factor receptors. A third approach to treat cancer exploits mounting information implicating the important contribution of the microenvironments within which tumor cells develop, proliferate, and (in the case of metastasis) colonize and occupy distant sites. Such strategies include inhibiting new vasculature and augmenting immune system responses.

Each of the above categories of cancer treatments includes agents that are capable of markedly suppressing tumor growth, but each also suffers from failures due to the engagement or selection of resistance programs. Tumor-cell–autonomous or intrinsic resistance mechanisms such as the activation of multidrug resistance efflux pumps, activation of bypass signaling pathways, and secondary mutations in drug targets are well established, and designs of therapeutics have iteratively evolved to exploit these molecular alterations. Less well studied are factors that contribute to cell-nonautonomous or extrinsic mediators of therapy resistance, such as those provided by nonmalignant cells and structural constituents of the tumor microenvironment. Recent work has defined niches within tissues and organs that offer sanctuary to tumors and activate therapy resistance programs. In several notable instances, efforts to exploit these tumor–host dynamics have led to successful clinical translation to affect patient survival. Here we discuss mechanisms by which tumor and host interactions in the microenvironment influence treatment resistance, with an emphasis on reactions and responses induced by the cancer therapeutics themselves that have the potential to attenuate treatment lethality and paradoxically promote tumor cell survival.

Authors' Affiliations: [1]Division of Human Biology, Fred Hutchinson Cancer Research Center, and [2]School of Medicine, University of Washington, Seattle, Washington

Corresponding Author: Peter S. Nelson, Division of Human Biology, Fred Hutchinson Cancer Research Center, 1100 Fairview Avenue North, MS D4-100, Seattle, WA 91809. Phone: 206-667-3377; Fax: 206-667-2917; E-mail: pnelson@fhcrc.org

doi: 10.1158/1078-0432.CCR-11-0768

Published OnlineFirst May 22, 2012; DOI: 10.1158/1078-0432.CCR-11-0768

Therapy Resistance

Tumor microenvironment

Neoplasms arise and grow in complex and dynamic ecosystems. For most types of solid tumors, the microenvironment is comprised of numerous resident benign cell types derived from distinct developmental lineages, as well as nonresident cell types that may be transient or may persist to become permanent components of an evolving interactive bionetwork. A structural framework provided by insoluble matrix proteins and gradients of diffusible growth factors, hormones, oxygen, reactive oxygen species, and nutrients adds to the complexity.

Of importance, many facets of the tumor microenvironment are capable of profoundly influencing the behavior of preneoplastic and overtly malignant cells. In contrast with fibroblasts derived from benign tissues, cancer-associated fibroblasts can augment the growth of preneoplastic cells and influence invasive tumor behavior in a number of organs, including the prostate, breast, and stomach (1–3). Likewise, inflammatory cell components such as B cells, T cells, and macrophages can promote adverse cancer phenotypes within the skin, breast, and other tissues (4, 5). The existence of a temporally dynamic microenvironment is evident in studies such as those showing that a normal young liver microenvironment is tumor suppressive, whereas a normal aged liver microenvironment is permissive for tumor establishment and progression (6). Similarly, detailed studies of tumor hypoxia, pH, angiogenesis, and rigidity have clearly shown that these and other attributes of the microenvironment can produce major changes in tumor phenotypes.

Although recent findings emphasize the importance of studying tumor characteristics, such as proliferation and invasion, in the context of the multidimensional influences exerted by the tumor microenvironment, there is less information concerning the roles played by the microenvironment in resistance to cancer therapeutics. However, it is well recognized that *ex vivo* assays of chemotherapeutics poorly recapitulate *in vivo* effectiveness (7). In part, these differences clearly reflect drug delivery issues related to vascular access, interstitial pressures, and metabolism (8). However, other elements of the tumor microenvironment can affect tumor phenotypes to augment drug resistance. Distinct microenvironments can provide niches that contribute substantially to tumor cell survival and eventual relapse and therapy failure. A few examples serve to illustrate the variety of ways in which the context provided by the tumor microenvironment can influence tumor resistance to therapeutics (for reviews, see refs. 8–10), as described below.

Therapy resistance mediated by soluble factors. As with chronic myelogenous leukemia (CML), Philadelphia chromosome-positive acute lymphocytic leukemia (Ph^+ALL) is driven by the BCR-ABL fusion protein and is sensitive to the Abl tyrosine kinase inhibitor imatinib (11). In a series of experiments reported by Williams and colleagues (12), a mouse model of Ph^+ALL was developed that exhibited resistance to imatinib, although Abl kinase activity was inhibited by drug treatment. However, tumor cells isolated from this model were still sensitive to imatinib *in vitro*, supporting the hypothesis that components of the host microenvironment (in this case, the hematopoietic microenvironment) promote resistance. Through further experimentation, host cytokines, such as interleukin (IL)-7, were determined to promote growth despite imatinib treatment (12). Other studies implicated galectin 3 induction in CML by the bone marrow microenvironment as a contributing factor to drug resistance and long-term lodgment of leukemic cells in the bone marrow niche (13). Further evidence for this mechanism of therapy resistance (described below) points to the role(s) of cancer therapeutics themselves in promoting the production of microenvironment-derived soluble factors.

Therapy resistance mediated by physical barriers. Cancers that arise from pancreatic duct cells are highly lethal and show quite limited responses to radiation or chemotherapy. However, cell lines and xenografted tumors derived from pancreatic cancers do exhibit responses to many chemotherapeutic drugs, such as gemcitabine, an agent used commonly to treat pancreatic cancer patients with modest efficacy (14). In a series of insightful studies using the KDM genetically engineered model of pancreatic cancer, Olive and colleagues (15) found a marked difference between tumor cells grafted into subcutaneous sites and cancers arising within the environment of the *in situ* pancreas in terms of responses to chemotherapy. They also found that major contributors to these differential tumor responses were limited vascularization and poor perfusion, which constrained drug penetration within the pancreas. The efficacy of chemotherapy was substantially enhanced through the use of IPI-926, a sonic hedgehog pathway inhibitor that depleted tumor-associated stromal tissue, increased tumor vascularity, increased intratumoral chemotherapy concentrations, and consequently inhibited tumor growth (15).

Therapy resistance influenced by cell adhesion. Physical interactions between multiple-myeloma cells and structural constituents of the bone marrow have been shown to profoundly influence *de novo* and acquired resistance to chemotherapy (16). Mechanisms that contribute to adhesion-mediated resistance include tumor-cell binding—via integrins and other components—to ligands on stromal cells and extracellular matrix such as fibronectin, collagens, and laminins. Consequent therapy resistance occurs through several pathways, including redistribution of the antiapoptotic proteins CASP8 and FADD-like apoptosis regulator from the cytoplasm to cell membranes, induced proteasomal degradation of the proapoptotic protein BCL2-interacting mediator of cell death, and transient posttranslational upregulation of the cyclin-dependent kinase inhibitor p27 (17, 18). Of importance, drug sensitivity can be augmented by agents that disrupt adhesion. In preclinical studies, a blocking antibody to α4 integrin reduced tumor burden and increased overall survival in a mouse model of multiple myeloma, and dramatically augmented myeloma responses when used in conjunction with melphalan, a

Published OnlineFirst May 22, 2012; DOI: 10.1158/1078-0432.CCR-11-0768

drug in common clinical use for the treatment of multiple myeloma (19). Information about the key relationships between myeloma cells and the bone marrow microenvironment led to a series of rationally designed clinical trials that cotargeted tumor and microenvironment interactions. Lenalidomide, an agent that among other effects decreases tumor cell binding to bone marrow components, and bortezomib, a proteosome inhibitor that among other effects downregulates adhesion molecules on both tumor cells and bone marrow stroma, were both shown to substantially improve overall survival (20), and these agents are now part of the routine clinical management of patients with multiple myeloma.

Microenvironment reactions to cancer-directed therapeutics

It is important to consider that the effects of most cancer-directed therapeutics are not entirely restricted to neoplastic cells, and that such therapeutics can also interact with—and alter—benign cells in local and distant host microenvironments. The potential for such effects is particularly relevant for nonspecific treatments involving ionizing radiation and genotoxic drugs. Highly conserved damage and stress-response programs have evolved to prevent the propagation of oncogenic genetic damage to progeny by temporarily arresting cell growth for DNA repair, or irreversibly arresting growth through senescence or apoptosis.

DNA damage response. The DNA damage response (DDR) is a complex and coordinated process that occurs following a breach in the integrity of DNA (21). The DDR likely evolved to protect the host from cells that sustain irreversible genomic damage resulting from exposure to exogenous and endogenous genotoxins. The DDR culminates in the elimination of cells whose damage cannot be repaired. Common routine environmental insults and byproducts of cellular metabolism produce in excess of 1 million individual DNA lesions per cell per day (22). To deal with this assault, repair mechanisms are in continual operation, and the rate of repair is sufficient to manage the rate of damage. However, exposure to genotoxic cancer therapeutics produces damage that far exceeds the capacity of the repair process to maintain DNA integrity. Alkylating agents produce DNA interstrand cross-links, which promote DNA double-strand breaks. Topoisomerase inhibitors produce several effects, including the generation of interstrand cross-links, the creation of free radicals, and the stabilization of DNA with consequent inhibition of proper DNA replication and a consequent damage response signal. Platinum drugs induce DNA adducts and double-strand breaks, and the antibiotic bleomycin induces direct double-strand breaks. These and other chemotherapeutics engage the DDR to initiate fail-safe programs that result in permanent growth arrest (senescence) or the execution of cell death (apoptosis).

The DDR is enacted by the Mre11-Rad50-Nbs1 mediator complex, which denotes specific sites of damage, followed by a second phase that propagates the recognition signal to ultimately influence repair and cellular phenotypic responses. The DDR progresses through a signaling cascade that includes ATR and ATM (23). In the context of double-strand breaks resulting from chemotherapy, ATM autophosphorylates at multiple sites, self-activates, and instigates reactions that assemble checkpoint proteins such as p53BP1 and BRCA1 at the break site to promote damage repair (24–26). Concurrently, ATM activates CHK2, leading to the stabilization and accumulation of p53, a pivotal mediator of either pause and repair or permanent growth arrest and cell death. Although tumor cells commonly inactivate key components of the DDR program, benign cells of the tumor microenvironment are fully capable of producing robust responses to genotoxic stress. It has recently become apparent that in addition to the cell-autonomous components of the DDR that influence the damaged cell itself, the DDR also promotes a cell-nonautonomous program of secreted factors that are capable of affecting numerous cell types comprising the tumor microenvironment, including those tumor cells that have survived the first salvo of chemotherapy and radiotherapy.

DNA damage secretory program. The secretory phenotype of damaged cells was first reported in the context of cellular senescence, a state of permanent growth arrest. Cellular senescence, as described by Hayflick and Moorehead (27) in the context of replicative exhaustion, is associated with characteristic morphologic features encompassing enlarged flattened cell bodies with increased cytoplasmic granularity. Although their growth has been arrested, senescent cells remain viable and metabolically active (28). The mechanism behind replicative exhaustion involves the progressive erosion of telomeres after many replication cycles, with the consequent induction of a DDR-like response culminating in the induction of the CDK inhibitors p21 and p16 and permanent growth arrest (29). Investigators have identified several other inducers of senescence, including oxidative stress and reactive oxygen species, activation of specific oncogenes such as *RAS* and *BRAF* (30, 31), and profound levels of DNA damage, such as those encountered in the context of chemotherapy and radiotherapy.

Detailed studies of senescent cells revealed that this state is accompanied by the production and secretion of a remarkable spectrum of cytokines, growth factors, and proteases, many of which have been shown to play roles in promoting tumor growth and invasion (32–34). Collectively, these secreted factors have been termed a senescence-associated secretory phenotype (35) or senescence-messaging secretome (36). However, it appears that a full senescence phenotype is not required for components of this secretory program to be engaged; rather, cell stress and DNA damage are the central initiators. This concept broadens the description of these largely overlapping programs to include the acute stress-associated phenotype (37) and DNA damage-associated secretory program (DDSP). Deep discovery-driven analyses of transcript and protein responses to genotoxic stress induced by cancer therapeutics have identified several hundred factors derived from benign cells comprising the tumor microenvironment (32, 38, 39).

Published OnlineFirst May 22, 2012; DOI: 10.1158/1078-0432.CCR-11-0768

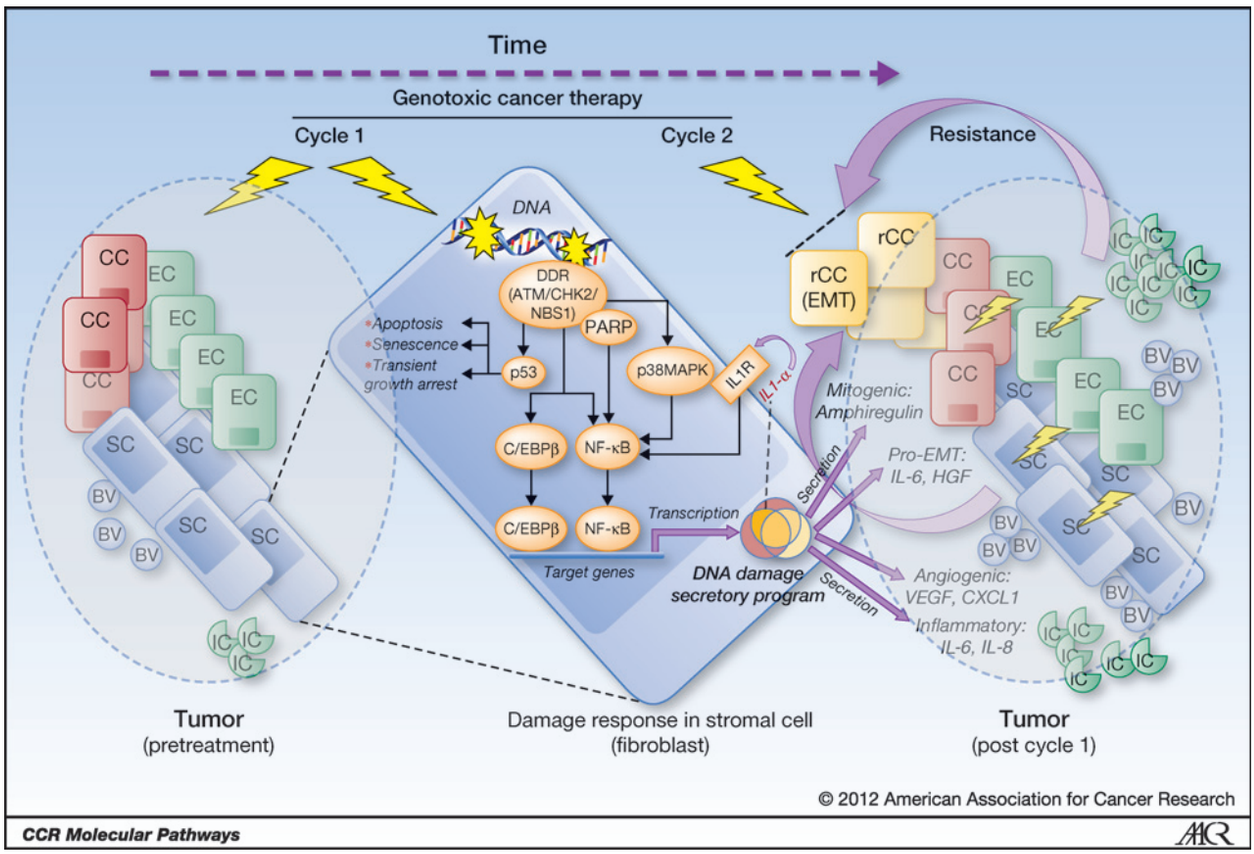

Figure 1. Therapy resistance is promoted by genotoxic treatment-induced damage responses in the tumor microenvironment. The local environment in which most neoplasms originate is a complex ecosystem comprised of cancer cells, benign resident cells, and transient cells (e.g., inflammatory cell types), as well as additional structural and soluble components. Genotoxic cancer therapeutics induce DNA damage in tumor cells, leading to cell death or senescence, but can also induce genotoxic stress in benign cells, such as tumor-associated fibroblasts comprising the tissue stroma. DNA damage and other stressors initiate damage response programs, such as the DDR, with several effector arms, including the generation and secretion of a diverse spectrum of cytokines, growth factors, and proteases (here denoted the DDSP). Individual components of the DDSP are well known to promote inflammation, angiogenesis, epithelial-to-mesenchymal transition, and tumor cell proliferation, and to augment resistance to cancer therapeutics. Targeting individual DDSP components or key upstream master regulators (e.g., NF-κB, p38MAPK, and PARP) may enhance the effectiveness of commonly used antineoplastic agents by suppressing microenvironment-derived resistance mechanisms. BV, blood vessel, CC, cancer cell; EC, epithelial cell; IC, inflammatory cell; rCC, resistant cancer cell; SC, stromal cell.

The composition of the DDSP is complex and includes proinflammatory cytokines such as IL-6 and IL-8, extracellular matrix–altering proteases, proneurogenic factors, angiogenic growth factors, and epithelial mitogens that include agonists for the epidermal growth factor receptor (EGFR), such as amphiregulin and epiregulin (38, 39). These cell-nonautonomous effectors of the stress-response program likely evolved to propagate a tissue-damage signal locally and distantly in order to enhance the elimination of damaged cells through immune clearance, and hasten repair through angiogenesis and the migration and proliferation of epithelial and stromal cells. However, in the setting of a malignancy, where neoplastic cells co-opt such microenvironment cues, such effects may have adverse consequences. Individual components of the DDSP can suppress apoptosis and enhance the proliferation of premalignant and malignant epithelium (34), stimulate migration and invasion (38, 39), and transition epithelial cells to acquire mesenchymal phenotypes (38) with augmented resistance to chemotherapy and radiation (Fig. 1; ref. 40).

Findings from several preclinical studies support the concept that treatment-induced microenvironment damage can promote adverse tumor outcomes. Recent work using modern tools of molecular biology recapitulated the insightful studies carried out in the 1950s by Revesz (41), who enhanced the growth of transplanted allogeneic and syngeneic tumors by combining lethally irradiated tumor cells with nonirradiated tumor cells. This so-called Revesz effect was later shown to be due to the metabolic activities of the irradiated cells resulting in the production of diffusible factors that conditioned the tumor microenvironment (42, 43). More recently, using a mouse model of breast carcinoma, Nguyen and colleagues (44) determined that ionizing radiation acting on the breast microenvironment accelerated the development of aggressive p53-null breast cancers. The development of these tumors was found to be influenced by TGF-β signaling and exhibited distinct

Published OnlineFirst May 22, 2012; DOI: 10.1158/1078-0432.CCR-11-0768

molecular programs involving estrogen receptor and stem cell activity. Similar results were reported in studies of myogenic cells, in which implanted cells rapidly progressed to poorly differentiated tumors in irradiated muscle microenvironments relative to cells implanted into nonirradiated muscle (45). Tumorigenicity was also found to be dependent on the dose of preirradiation and to vary depending on the host's genetic background. Whether such damaged microenvironments would also promote therapy resistance has not been tested.

Studies using genotoxic chemotherapeutics have extended these observations to show that treatment-induced damage to the microenvironment can promote a chemoresistant niche of residual disease that subsequently serves as the nidus for relapse. In experiments using doxorubicin to treat the Eμ-Myc model of transplantable lymphoma, Gilbert and Hemann (37) determined that the surviving metastatic tumor cells were exclusively localized to the thymus. Detailed molecular analyses of damage responses in different lymphoid tissues and of individual cell types comprising these tissues identified IL-6 and Timp-1 as prosurvival factors secreted selectively by thymic endothelial cells. Tumor-cell resistance was shown to be due to the paracrine production of IL-6 and Timp-1, and inhibition of these factors, or the upstream signaling pathway operating through p38 mitogen-activated protein kinase (p38MAPK), enhanced the effectiveness of subsequent chemotherapy (37). In addition to providing proof-of-principle that damage induced by cancer therapeutics to residents of the tumor microenvironment can influence tumor behavior (in this case, therapy responses), this study showed that different tissues, and indeed the distinct cell types that comprise these tissues, have varied damage responses, a finding that has important implications for designing clinical trials to exploit these results.

Clinical–Translational Advances

Therapeutic context

The concept of developing treatment strategies to modify the tumor microenvironment or interrupt interactions between tumor cells and components of the microenvironment is attractive for several reasons. First, this approach has been applied successfully in several malignant diseases, as exemplified most strikingly in multiple myeloma, where cotargeting the tumor microenvironment is now a mainstay of the overall treatment paradigm (20). Second, there are many potential ways to influence the tumor microenvironment to ensure more effective tumor-cell killing, ranging from mobilizing tumor cells [e.g., via CXCR4/CXCL12 axis blockade (46)] to breaking down desmoplastic barriers for more efficient drug penetration (15). Third, because the tumor microenvironment targets are generally derived from benign cells involving well-conserved developmental pathways, they are unlikely to be subject to mutation and resistance. Fourth, most tumor microenvironment targets represent a non–cross-reactive feature of the tumor that may not contribute substantially to toxicity.

In treatment-induced therapy resistance, it is important to consider that context is critical: The treatment itself can unmask or induce new opportunities for intervention. Unfortunately, the standard regimens that are currently used to treat most solid tumors are ideally suited to promote microenvironment-mediated resistance. Most chemotherapeutics are dosed in a sequence of treatment cycles that are generally designed to allow normal host tissues and organs to recover and avoid major morbidity and host lethality. Radiotherapy is similarly administered in a series of fractionated doses at intervals spanning days to weeks. Initial cycles of treatment can eliminate a substantial percentage of the tumor cell mass, but they can also induce a damage response in cells that constitute the tumor microenvironment (Fig. 1). Tumor cells that survive the first salvos of therapy are thus exposed to the high levels of growth factors, cytokines, and proteases that comprise the DDSP and are capable of bolstering the remaining tumor cells to survive subsequent treatment cycles. In the murine lymphoma studies described above (37), key prosurvival factors such as IL-6 and Timp-1 emerged as therapeutic targets only in the context of treatment, whereas without genotoxic stress, suppression of these factors was not relevant. The progrowth, prosurvival, and proangiogenic components of the DDSP may also underlie the accelerated tumor repopulation kinetics that have been observed during intervals between treatments and account for rapid tumor repopulation, an important cause of treatment failure (47).

Cotargeting specific microenvironment effectors

The robust induction of growth factors and cytokines by DNA-damaging therapeutics may be a contributing factor in the limited responses observed in clinical studies of targeted therapeutics, such as those designed to inhibit angiogenesis or suppress EGF signaling. Following genotoxic treatments, small-molecule inhibitors and receptor-directed antibodies must contend with very high local treatment-induced concentrations of ligands for these receptors, such as VEGF, amphiregulin, and epiregulin. Recognizing that multiple distinct ligands may activate redundant signaling programs to resist these targeted treatments is the initial step in designing the appropriate clinical studies to confirm effective pathway suppression. Although it is remarkably diverse (36, 38), the secretory program induced by DNA damage and the attendant cell stress is not unlimited, and it is likely that only a subset of the program effectively contributes to therapy resistance. Further, components of the DDSP may assist in controlling tumor growth through host damage response signaling that attracts inflammatory cells and engages other tissue repair processes. Thus, a reasonable strategy would be to identify and cotarget only the key DDSP factors that are responsible for inducing a therapy-resistant phenotype.

Cotargeting the collective DDSP

An alternative to targeting individual resistance-promoting components of the DDSP, which may require multiple drugs deployed in combination to effectively suppress

Published OnlineFirst May 22, 2012; DOI: 10.1158/1078-0432.CCR-11-0768

particular paracrine interactions, would be to inhibit the master regulators that transduce the DDR signal to modulate the expression of large subsets of effector proteins. Although this system is complex and incompletely understood, current knowledge about the DDR suggests several nodes that could be evaluated (Fig. 1). For example, inhibition of p38MAPK has been shown to suppress the secretion of most stress-responsive secretory proteins in fibroblasts (35), primarily through NF-κB, which is also an attractive target in the context of regulating DDR-induced responses. PARP-1 has been shown to be activated in response to DNA damage and to propagate a signaling cascade that includes the production of a secretome with protumoral and prometastatic properties (48). Thus, PARP-1 inhibitors, which are currently in clinical trials for the treatment of breast and ovarian cancers, could be repurposed for inhibiting the microenvironment DDSP in the context of genotoxic tumor therapy. IL-1α, itself a component of the damage-associated program, has been shown to promote the secretion of several key proinflammatory cytokines via interaction with cell-surface IL-1R and consequent activation of NF-κB (49). It is likely that additional master regulators of the DDSP will be identified as our knowledge about the signal transduction program matures.

Conclusions

Many questions remain regarding the optimal strategies for effectively suppressing the prosurvival microenvironment induced directly by cancer therapeutics. The extent to which damage-associated secretory responses vary among different organs, different cell types within tissues, and different individuals—and how this variation is controlled—remains unclear. Such information may be quite important when considering microenvironment targets in different primary tumor locations and sites of metastatic disease. The systemic effects of DNA-damage responses also likely influence the resistance of tumor cells to treatment. The duration or persistence of damage-associated paracrine activity has also not been established, and this may be quite important for designing clinical trials that sequence genotoxic agents with agents that inhibit microenvironment factors, and for understanding therapy-resistant niches and tumor-cell dormancy and reactivation. Intuitively, it seems that suppressing the damage response prior to genotoxic treatment would be ideal. Sequencing microenvironment agents between intervals of genotoxic therapy is also a reasonable approach and is analogous to metronomic designs in which cytotoxic agents are alternated with cytostatic drugs to inhibit rapid tumor repopulation (50).

It is becoming clear that context (in this case, the microenvironment) profoundly influences tumor-cell behaviors, including treatment resistance. Of importance, this bionetwork is dynamic, and for every action, such as exposure to genotoxic stress, there are reactions and consequences throughout the micro- and macrosystems. Defining the interactions among tumor cells, benign constituents of the tumor, and the influences of treatment will likely yield more effective combinatorial strategies that improve upon conventional approaches that heretofore have focused primarily on the neoplastic cell.

Disclosure of Potential Conflicts of Interest

No potential conflicts of interest were disclosed.

Authors' Contributions

Conception and design: P.S. Nelson
Development of methodology: Y. Sun, P.S. Nelson
Acquisition of data (provided animals, acquired and managed patients, provided facilities, etc.): Y. Sun
Analysis and interpretation of data (e.g., statistical analysis, biostatistics, computational analysis): Y. Sun
Writing, review, and/or revision of the manuscript: Y. Sun, P.S. Nelson

Acknowledgments

The authors thank Judy Campisi and members of the Nelson laboratory for helpful discussions.

Grant Support

National Cancer Institute, National Institutes of Health (grants U54CA126540, U01CA164188, and R01CA165573); Prostate Cancer Foundation.

Received December 3, 2011; revised March 10, 2012; accepted March 27, 2012; published OnlineFirst May 22, 2012.

References

1. Olumi AF, Grossfeld GD, Hayward SW, Carroll PR, TIsty TD, Cunha GR. Carcinoma-associated fibroblasts direct tumor progression of initiated human prostatic epithelium. Cancer Res 1999;59:5002–11.
2. Allinen M, Beroukhim R, Cai L, Brennan C, Lahti-Domenici J, Huang H, et al. Molecular characterization of the tumor microenvironment in breast cancer. Cancer Cell 2004;6:17–32.
3. Quante M, Tu SP, Tomita H, Gonda T, Wang SS, Takashi S, et al. Bone marrow-derived myofibroblasts contribute to the mesenchymal stem cell niche and promote tumor growth. Cancer Cell 2011;19:257–72.
4. Andreu P, Johansson M, Affara NI, Pucci F, Tan T, Junankar S, et al. FcRgamma activation regulates inflammation-associated squamous carcinogenesis. Cancer Cell 2010;17:121–34.
5. Denardo DG, Brennan DJ, Rexhepaj E, Ruffell B, Shiao SL, Madden SF, et al. Leukocyte complexity predicts breast cancer survival and functionally regulates response to chemotherapy. Cancer Discov 2011;1:54–67.
6. McCullough KD, Coleman WB, Smith GJ, Grisham JW. Age-dependent induction of hepatic tumor regression by the tissue microenvironment after transplantation of neoplastically transformed rat liver epithelial cells into the liver. Cancer Res 1997;57:1807–13.
7. Green SK, Frankel A, Kerbel RS. Adhesion-dependent multicellular drug resistance. Anticancer Drug Des 1999;14:153–68.
8. Trédan O, Galmarini CM, Patel K, Tannock IF. Drug resistance and the solid tumor microenvironment. J Natl Cancer Inst 2007;99:1441–54.
9. Minchinton AI, Tannock IF. Drug penetration in solid tumours. Nat Rev Cancer 2006;6:583–92.
10. Meads MB, Gatenby RA, Dalton WS. Environment-mediated drug resistance: a major contributor to minimal residual disease. Nat Rev Cancer 2009;9:665–74.

Published OnlineFirst May 22, 2012; DOI: 10.1158/1078-0432.CCR-11-0768

11. Talpaz M, Shah NP, Kantarjian H, Donato N, Nicoll J, Paquette R, et al. Dasatinib in imatinib-resistant Philadelphia chromosome-positive leukemias. N Engl J Med 2006;354:2531–41.
12. Williams RT, den Besten W, Sherr CJ. Cytokine-dependent imatinib resistance in mouse BCR-ABL+, Arf-null lymphoblastic leukemia. Genes Dev 2007;21:2283–7.
13. Yamamoto-Sugitani M, Kuroda J, Ashihara E, Nagoshi H, Kobayashi T, Matsumoto Y, et al. Galectin-3 (Gal-3) induced by leukemia microenvironment promotes drug resistance and bone marrow lodgment in chronic myelogenous leukemia. Proc Natl Acad Sci U S A 2011;108:17468–73.
14. Shimamura T, Royal RE, Kioi M, Nakajima A, Husain SR, Puri RK. Interleukin-4 cytotoxin therapy synergizes with gemcitabine in a mouse model of pancreatic ductal adenocarcinoma. Cancer Res 2007;67:9903–12.
15. Olive KP, Jacobetz MA, Davidson CJ, Gopinathan A, McIntyre D, Honess D, et al. Inhibition of Hedgehog signaling enhances delivery of chemotherapy in a mouse model of pancreatic cancer. Science 2009;324:1457–61.
16. Meads MB, Hazlehurst LA, Dalton WS. The bone marrow microenvironment as a tumor sanctuary and contributor to drug resistance. Clin Cancer Res 2008;14:2519–26.
17. Shain KH, Landowski TH, Dalton WS. Adhesion-mediated intracellular redistribution of c-Fas-associated death domain-like IL-1-converting enzyme-like inhibitory protein-long confers resistance to CD95-induced apoptosis in hematopoietic cancer cell lines. J Immunol 2002;168:2544–53.
18. Hazlehurst LA, Damiano JS, Buyuksal I, Pledger WJ, Dalton WS. Adhesion to fibronectin via beta1 integrins regulates p27kip1 levels and contributes to cell adhesion mediated drug resistance (CAM-DR). Oncogene 2000;19:4319–27.
19. Mori Y, Shimizu N, Dallas M, Niewolna M, Story B, Williams PJ, et al. Anti-alpha4 integrin antibody suppresses the development of multiple myeloma and associated osteoclastic osteolysis. Blood 2004;104:2149–54.
20. Anderson KC. Oncogenomics to target myeloma in the bone marrow microenvironment. Clin Cancer Res 2011;17:1225–33.
21. Zhou BB, Elledge SJ. The DNA damage response: putting checkpoints in perspective. Nature 2000;408:433–9.
22. Lodish HBA, Matsudaira P, Kaiser CA, Krieger M, Scott MP, Zipursky SL, et al. Molecular Biology of the Cell. 5th ed. New York: W.H. Freeman; 2004.
23. Durocher D, Jackson SP. DNA-PK, ATM and ATR as sensors of DNA damage: variations on a theme? Curr Opin Cell Biol 2001;13:225–31.
24. Huen MS, Chen J. The DNA damage response pathways: at the crossroad of protein modifications. Cell Res 2008;18:8–16.
25. Mailand N, Bekker-Jensen S, Faustrup H, Melander F, Bartek J, Lukas C, et al. RNF8 ubiquitylates histones at DNA double-strand breaks and promotes assembly of repair proteins. Cell 2007;131:887–900.
26. Stucki M, Jackson SP. gammaH2AX and MDC1: anchoring the DNA-damage-response machinery to broken chromosomes. DNA Repair (Amst) 2006;5:534–43.
27. Hayflick L, Moorhead PS. The serial cultivation of human diploid cell strains. Exp Cell Res 1961;25:585–621.
28. Shelton DN, Chang E, Whittier PS, Choi D, Funk WD. Microarray analysis of replicative senescence. Curr Biol 1999;9:939–45.
29. Collado M, Blasco MA, Serrano M. Cellular senescence in cancer and aging. Cell 2007;130:223–33.
30. Serrano M, Lin AW, McCurrach ME, Beach D, Lowe SW. Oncogenic ras provokes premature cell senescence associated with accumulation of p53 and p16INK4a. Cell 1997;88:593–602.
31. Michaloglou C, Vredeveld LC, Soengas MS, Denoyelle C, Kuilman T, van der Horst CM, et al. BRAFE600-associated senescence-like cell cycle arrest of human naevi. Nature 2005;436:720–4.
32. Bavik C, Coleman I, Dean JP, Knudsen B, Plymate S, Nelson PS. The gene expression program of prostate fibroblast senescence modulates neoplastic epithelial cell proliferation through paracrine mechanisms. Cancer Res 2006;66:794–802.
33. Rodier F, Coppé JP, Patil CK, Hoeijmakers WA, Muñoz DP, Raza SR, et al. Persistent DNA damage signalling triggers senescence-associated inflammatory cytokine secretion. Nat Cell Biol 2009;11:973–9.
34. Krtolica A, Parrinello S, Lockett S, Desprez PY, Campisi J. Senescent fibroblasts promote epithelial cell growth and tumorigenesis: a link between cancer and aging. Proc Natl Acad Sci U S A 2001;98:12072–7.
35. Freund A, Patil CK, Campisi J. p38MAPK is a novel DNA damage response-independent regulator of the senescence-associated secretory phenotype. EMBO J 2011;30:1536–48.
36. Kuilman T, Peeper DS. Senescence-messaging secretome: SMS-ing cellular stress. Nat Rev Cancer 2009;9:81–94.
37. Gilbert LA, Hemann MT. DNA damage-mediated induction of a chemoresistant niche. Cell 2010;143:355–66.
38. Coppé JP, Patil CK, Rodier F, Sun Y, Muñoz DP, Goldstein J, et al. Senescence-associated secretory phenotypes reveal cell-nonautonomous functions of oncogenic RAS and the p53 tumor suppressor. PLoS Biol 2008;6:2853–68.
39. Kuilman T, Michaloglou C, Vredeveld LC, Douma S, van Doorn R, Desmet CJ, et al. Oncogene-induced senescence relayed by an interleukin-dependent inflammatory network. Cell 2008;133:1019–31.
40. McConkey DJ, Choi W, Marquis L, Martin F, Williams MB, Shah J, et al. Role of epithelial-to-mesenchymal transition (EMT) in drug sensitivity and metastasis in bladder cancer. Cancer Metastasis Rev 2009;28:335–44.
41. Revesz L. Effect of tumour cells killed by x-rays upon the growth of admixed viable cells. Nature 1956;178:1391–2.
42. Seelig KJ, Revesz L. Effect of lethally damaged tumour cells upon the growth of admixed viable cells in diffusion chambers. Br J Cancer 1960;14:126–38.
43. van den Brenk HA, Crowe MC, Stone MG. Reactions of the tumour bed to lethally irradiated tumour cells, and the Révész effect. Br J Cancer 1977;36:94–104.
44. Nguyen DH, Oketch-Rabah HA, Illa-Bochaca I, Geyer FC, Reis-Filho JS, Mao JH, et al. Radiation acts on the microenvironment to affect breast carcinogenesis by distinct mechanisms that decrease cancer latency and affect tumor type. Cancer Cell 2011;19:640–51.
45. Morgan JE, Gross JG, Pagel CN, Beauchamp JR, Fassati A, Thrasher AJ, et al. Myogenic cell proliferation and generation of a reversible tumorigenic phenotype are triggered by preirradiation of the recipient site. J Cell Biol 2002;157:693–702.
46. Zeng Z, Shi YX, Samudio IJ, Wang RY, Ling X, Frolova O, et al. Targeting the leukemia microenvironment by CXCR4 inhibition overcomes resistance to kinase inhibitors and chemotherapy in AML. Blood 2009;113:6215–24.
47. Kim JJ, Tannock IF. Repopulation of cancer cells during therapy: an important cause of treatment failure. Nat Rev Cancer 2005;5:516–25.
48. Ohanna M, Giuliano S, Bonet C, Imbert V, Hofman V, Zangari J, et al. Senescent cells develop a PARP-1 and nuclear factor-kappaB-associated secretome (PNAS). Genes Dev 2011;25:1245–61.
49. Orjalo AV, Bhaumik D, Gengler BK, Scott GK, Campisi J. Cell surface-bound IL-1alpha is an upstream regulator of the senescence-associated IL-6/IL-8 cytokine network. Proc Natl Acad Sci U S A 2009;106:17031–6.
50. Shaked Y, Emmenegger U, Francia G, Chen L, Lee CR, Man S, et al. Low-dose metronomic combined with intermittent bolus-dose cyclophosphamide is an effective long-term chemotherapy treatment strategy. Cancer Res 2005;65:7045–51.